Assessing ADME properties of CJ-15,208: synthesis of new analogs and examination of P-glycoprotein interactions

By

Christianna Reedy

Submitted to the graduate degree program in Medicinal Chemistry and the Graduate Faculty of the University of Kansas in partial fulfillment of the requirements for the degree of Master of Science.

_____

Co-chairperson Jane V. Aldrich

_____

Co-chairperson Blake R. Peterson

_____

Teruna J. Siahaan

Date Defended: August 28, 2015

The Thesis Committee for Christianna Reedy

certifies that this is the approved version of the following thesis:

Assessing ADME properties of CJ-15,208: synthesis of new analogs and examination of P-glycoprotein interactions

_____

Co-chairperson Jane V. Aldrich

_____

Co-chairperson Blake R. Peterson

Date approved: September 4, 2015

Abstract

We are exploring analogs of the macrocyclic tetrapeptide natural product CJ-15,208 (*cyclo*[Phe-D-Pro-Phe-Trp]) as both potential analgesics and kappa opioid receptor (KOPr) antagonists. KOPr agonists exhibit analgesic activity but do not cause some of the adverse side effects associated with mu opioid agonists. Additionally, both KOPr agonists and antagonists have demonstrated the ability to block reinstatement of cocaine-seeking behavior under different conditions. CJ-15,208 has shown both opioid agonist (antinociceptive) activity and KOPr antagonist activity *in vivo*, while its D-Trp isomer, [D-Trp]CJ-15,208, has shown predominantly KOPr antagonist activity *in vivo*. Both compounds penetrate the central nervous system following oral administration and are stable to proteases in plasma and whole blood. However, studies in liver microsomes suggest that these peptides are susceptible to CYP P450 metabolism. Analogs of CJ-15,208 with modification on one of the aromatic residues were synthesized to study and improve pharmacokinetic properties. Additionally, CJ-15,208 and [D-Trp]CJ-15,208 were studied with *in vitro* biological barrier models using Madin-Darby canine kidney (MDCK) cells, both wild type and a line transfected with the MDR1 gene coding for the efflux protein P-glycoprotein (P-gp). The peptides' inhibition of P-gp was assessed using rhodamine 123 efflux, and their efflux was assessed by analyzing bidirectional transport across MDCK-MDR1 and MDCK-WT monolayers. Evidence of efflux was observed for CJ-15,208 in the transport studies, but the similar results in the experiments using MDCK-MDR1 and MDCK-WT cells make it unclear which efflux proteins are involved. Preliminary studies suggested that [D-Trp]CJ-15,208 may also be an efflux substrate, but additional studies are need to confirm this. The results of these studies will help guide the design and evaluation of new analogs of these lead peptides.

Acknowledgements

This dissertation is the product of my three years of study on the Department of Medicinal Chemistry of Kansas University, Lawrence, KS. I would like to thank many people who have helped me during my time in graduate school. First and foremost, I would like to thank my advisor, Dr. Jane V. Aldrich for her guidance and support even during a time of challenging transition. Her insight has helped developed my critical thinking and communication skills.

I would also like to thank all our lab members on Jane's laboratory for their support and encouragement: Previous lab member Dr. Sanjeewa N. Senadheera for his expertise and training in macrocyclic tetrapeptide synthesis and purification and for supplying CJ-15,208, [D-Trp]CJ-15,208, and the internal standard for the delivery studies; Dr. Archana Mukhopadhyay for her expertise and training in cell culture; Dr. Tanvir Khaliq for his training and help with the LC-MS/MS analysis as well as his previous work on the metabolism of the macrocyclic tetrapeptides; Dr. Tatyana Yakovleva and Dr. Dimitry Yakovleva for their expertise and training in analytical methods as well as general laboratory and safety procedure; Solomon A. Gisemba for always supplying me with a laugh and encouraging word; and Dr. Michael Ferracane for his ongoing work in modeling our peptide's interactions with the kappa opioid receptor. I would also like to thank Dr. Anand Joshi, a previous graduate student in Jane's laboratory, for his initial work on the transport of CJ-15,208.

I am very grateful for having excellent thesis committee members, Drs. Blake Peterson and Teruna J. Siahaan, for sharing their knowledge and giving me encouragement. Special thanks to Dr. Siahaan and his lab for giving me valuable comments on MDCK cells and transport experiments.

I would also like to thank the following people: Dr. Jay P McLaughlin and his group at the Torrey Pines Institute for Molecular Studies for performing the pharmacological assays and interpreting the data, Drs. Todd D. Williams and Lawrence L. Seib from the KU Mass Spectrometry Laboratory for their help analyzing the UPLC-MS/MS data, and Dr. Susan M. Lunte for allowing me to use her laboratory space.

I would like to extend my thanks to the Department of Medicinal Chemistry and its staff members for training and support. I'd also like to thank my professors who have taught me in this program. They have equipped me with the knowledge and skills I will need to be competitive in the field of medicinal chemistry. I am also grateful for the support I have received from the NIH-sponsored Biotechnology Predoctoral Training Program both financially and in my training,

A special thanks goes to my mother, Linda Lewis, and my brother, William Lewis for proving to me that it is possible to both survive graduate school and to be successful with a Master's degree. My husband has my eternal gratitude for his patience and support during the all night sessions in the laboratory and at the computer, as well as for his help and encouragement during every step of this journey. My thanks goes as well to the rest of my family members and my friends for cheering me on.

Finally, I would like to dedicate this dissertation to the faculty at the Department of Chemistry and Biochemistry at Abilene Christian University where I received my undergraduate degree. I would especially like to mention Dr. Eric Hardegree, who advised my undergraduate research and encouraged me to go to KU. The professors at ACU taught me to work hard and to remember that my worth is not dependent on score. I will always be grateful for what they contributed to my life.

Table of Contents

List of Tables

Page

List of Figures

Page

List of Schemes

Page

Abbreviations

ABC: ATP-binding cassette;

A-B: apical to basolateral;

BBB: blood-brain barrier;

BBMEC: bovine brain microvessel endothelial cell;

BCA: bicinchoninic acid;

BCRP: breast cancer resistant protein;

Boc: *tert*-butyloxycarbonyl;

B-A: basolateral apical;

CHOIR: manual multiple peptide synthesizer;

CNS: central nervous system;

CPP: conditioned place preference;

CSA: cyclosporin A;

CYP-P450: cytochrome P450;

DADLE: [D-Ala^2,Leu^5]enkephalin;

Dap: 2,3-diaminopropionic acid;

DCM: dichloromethane;

DIEA: *N*,*N*-diisopropylethylamine;

DMA: *N*,*N*-dimethylacetamide;

DMEM: Dulbecco's modified Eagle's medium;

DMF: *N*,*N*-dimethylformamide;

DMSO: dimethyl sulfoxide;

DOPr: delta opioid receptor;

DPDPE: *cyclo*[D-Pen^2,D-Pen^5]enkephalin;

DTT: dithiothreitol;

Dyn A: dynorphin A;

EDTA: ethylenediaminetetraacetic;

EGTA: ethylene glycol tetraacetic acid;

ESI-MS: electrospray ionization mass spectrometry;

ETOAc: ethyl acetate;

FBS: fetal bovine serum;

FDA: Food and Drug Administration;

Fmoc: 9-fluorenylmethoxycarbonyl;

Fmoc-OSu: 9-fluorenylmethyl *N*-succinimidyl carbonate;

GTPγS: guanosine-5'-(3-thiotriphosphate);

HATU: 2-(1H-7-azabenzotriazol-1-yl)-1,1,3,3-tetramethyluronium hexafluorophosphate;

HBSS: Hank's balanced salt solution;

HOBt: 1-hydroxybenzotriazole;

HPLC: high-performance liquid chromatography;

IAM: immobilized artificial membrane;

i.c.v.: intracerebroventricular;

i.p.: intraperitoneal;

i.t.: intrathecal;

JNK: c-Jun N-terminal kinase;

KOPr: kappa opioid receptor;

LC-ESI-MS/MS: liquid chromatography electrospray ionization tandem mass spectroscopy;

LY: lucifer yellow;

MDCK: Madin-Darby canine kidney;

MeCN: acetonitrile;

MeOH: methanol;

MOPr: mu opioid receptor;

MRM: multiple reaction monitoring;

Nle: norleucine;

NMP: *N*-methylpyrrolidone;

NOR: nociception receptor;

norBNI: nor-binaltorphimine;

PAMPA: parallel artificial membrane permeability assay;

P_{app}: apparent permeability coefficient;

PBS: phosphate-buffered saline;

P-gp: P-glycoprotein;

PMSF: phenylmethanesulfonylfluoride;

PNS: peripheral nervous system;

PTFE: polytetrafluoroethylene;

PVDF: P polyvinylidene difluoride;

RFU: relative fluorescence units;

PyBOP: benzotriazole-1-yloxytripyrrolidinophosphonium hexafluorophosphate;

Rh 123: rhodamine 123;

RP-UPLC: reversed phase ultra-high performance liquid chromatography;

SDS: sodium dodecyl sulfate;

s.c.: subcutaneous;

SAR: structure-activity relationship;

SPPS: solid-phase peptide synthesis;

TBS: tris-buffered saline;

TEER: transepithelial electrical resistance;

TFA: trifluoroacetic acid;

THF: tetrahydrofuran

TLC: thin layer chromatogram;

UPLC: ultra-performance liquid chromatography;

WT: wild type.

Chapter I: Literature Review

1.1 Therapeutic potential of polypeptides

Advances in technology have resulted in increasing identification of new potential drug targets. The completion of the human genome project in 2003 and the subsequent genome mining was widely expected to result in a radical increase in drug targets and new classes of drugs.[1] However, these new potential leads for drug design have not resulted in increases in the number of small molecule leads, with the registration of new chemical entities each year remaining relatively constant since 1980.[2] While medicinal chemists have more potential therapeutic targets than ever before, they also face higher standards for drug safety and efficacy. Additionally, many new therapeutic targets involve protein-protein or protein-peptide interactions that can be difficult to stimulate or inhibit with small molecules. Increasingly, the pharmaceutical industry is turning to macromolecules, including peptide and protein therapeutic agents, to overcome these obstacles. Table 1.1 lists some prominent benefits and challenges of therapeutic polypeptides.[3, 4]

Table 1.1: Therapeutic polypeptides: pros and cons

Pros	**Cons**
High selectivity	Proteolytic liability
Potency	Low membrane permeability
Low off-target interactions	Short half-life
Wide range of targets	Route of administration

Many pharmaceutically desirable aspects of polypeptides come from their unique structures. Peptides and proteins often have increased selectivity and specificity due to their large surface areas and potential for polar and non-polar interactions.[3] Most protein pockets have evolved to interact with complementary sequences of their endogenous peptide or protein

counterparts. Polypeptides also have multiple functionalities displayed in specific sequences that interfere with interaction with off-target proteins, conferring high selectivity. Peptides also are often very potent, activating the conformational changes in their targets required to initiate the desired activity. Polypeptides also are less likely to accumulate in tissues as they are often rapidly cleared by enzymatic degradation and renal elimination. These features make polypeptides desirable targets for the development of safe and potent therapeutics.

However, while peptides and proteins are an increasing share of the pharmaceutical market, they have been limited by delivery challenges. Most therapeutics approved by the Food and Drug Administration (FDA) are oral drugs. Oral delivery is attractive because it is less invasive and there can be increased ease of administration and compliance compared to injectable drugs.[5] However, the majority of polypeptide therapeutics are currently delivered via subcutaneous, intramuscular or intravenous routes. Other routes of administration being explored include transdermal, intranasal, and pulmonary delivery, but these strategies have their own drawbacks and limitations.[5]

One reason why polypeptides are often not orally bioavailable is their impermeability across biological barriers. The most commonly used guide for whether a compound will be orally bioavailable is Lipinski's "rule of five," which offers guidelines for predicting oral bioavailability of small-molecule drugs.[6] The rule states that molecules are more likely to be orally bioavailable if their properties fall within the following parameters: 1. A molecular weight of <500 Da; 2. The number of hydrogen bond donors ≤5; 3. The number of hydrogen bond acceptors ≤10; and 4. A log *P* not ≥5. A number of other variables can be added to this list,[7] and guidelines are even stricter for prediction of penetration into the Central Nervous System (CNS).[8]

Most polypeptides do not fall within the bounds of these rules. Peptides are often much larger than 500 Da, and their sizes can hinder their transport across cells, such as those composing

the intestinal and blood-brain barriers. Further, polypeptides typically have greater hydrogen bonding potential than is recommended by the rule of five, as hydrogen bond donors and acceptors are abundant in the peptide backbone and can be present in peptide side chains as well. High hydrogen bonding potential can increase the energy costs of passing through lipid membranes. However, these hydrogen bond donors and acceptors can also participate in intramolecular bonds, increasing the logP of some peptides. Polypeptides can show high logP values, as well as poor aqueous solubility, which also hinders their oral delivery. However, it should be noted that these guidelines were not generated based on data from therapeutic peptides, and while these properties can pose a challenge for oral delivery, they do not contradict it.

Another challenge to therapeutic use of polypeptides is their rapid clearance. Polypeptides, especially those of smaller size, are susceptible to rapid digestion by proteases present in the liver, kidneys, and blood.[4] This metabolic instability often leads to short half-lives (minutes) and limited exposure of polypeptides at their target tissues.

There has been increased interest in the development of orally bioavailable polypeptide therapeutics in recent years, and small peptides have seemed to exhibit the most potential in this category. While most polypeptides far exceed 500 Da, peptides of five amino acids or less can be within range of this target. Many currently approved peptide therapeutics are relatively small. Of the 65 peptide products with <50 amino acids that were on the market in 2010, almost half comprised only nine amino acids or less.[9] Further, peptides can potentially be made more orally bioavailable by cyclization. Peptide cyclization can mask their hydrogen bonding groups by forming reversible intramolecular hydrogen bonds, while allowing them to pass through lipid environments.[10] This allows macrocyclic peptides to be much more permeable through biological barriers.

One cyclic peptide in particular has been the subject of many permeability studies is cyclosporin A (CSA).[11-14] This 11-residue cyclic peptide is an orally bioavailable immunosuppressant drug, although it requires special formulation due to its low water solubility. This natural product has been used as a model for studying structural modifications that can be used to enhance oral bioavailability of other cyclic peptides.[10] CSA is a macrocyclic peptide, and studies comparing the membrane permeability of macrocyclic peptides to their linear counterparts suggest that macrocyclization can increase its membrane permeability by eliminating the charges due to N- and C- termini and decreasing polarity.[15] Studies also suggest that CSA's permeability likely benefits from multiple 3-dimensional conformations that it can adopt.[16]

The role of conformational flexibility in passive transport has been explored using a library of synthetic macrocyclic hexa- and heptapeptides screened computationally and in a parallel artificial membrane permeability assay (PAMPA).[16] Peptides that were able to adopt multiple conformations, masking their hydrogen bonding groups when in low-dielectric environments and exposing them in high-dielectric environments, had higher passive permeabilities than did more rigid peptides. In the proposed model, the hydrogen bonding groups in the peptide are exposed to the aqueous environment, increasing the peptide's water-solubility, but in the lipid bilayer intramolecular hydrogen bonds form, masking these groups during transport.

Other modifications, such as N-methylation of the amides, have also been shown to increase macrocyclic peptide permeability in cellular assays, likely by activating facilitated transport mechanisms. A library of 54 poly-alanine macrocyclic hexapeptides with different N-methylation patterns were screened using the PAMPA assay and using Caco-2 cell monolayers; the peptides with the highest permeability across Caco-2 cells were not permeable across PAMPA.[17] Caco-2 permeability appeared to be much more influenced by 3-dimensional structure than by lipophilicity.

These studies indicate that peptide bioavailability can be increased in some cases by cyclization and/or by reducing hydrogen bonding by replacing hydrogen bonding groups or forming intramolecular hydrogen bonds. Additionally, facilitated transport may be utilized by some peptides, but this mechanism is difficult to harness as the peptide's conformation seems to have substantial impact on facilitated transport.[18] Moreover, it is essential that such structural changes are not detrimental to the peptide's activity at its target.

1.2 The kappa opioid receptor as a therapeutic target and its small-molecule ligands

There are three opioid receptors, mu, kappa, and delta, and a related receptor, the nociception receptor (NOR).[19, 20] These receptors are in the superfamily of G protein coupled receptors, which are capable of producing a variety of downstream signaling and pharmacological effects. These receptors have been of great historical interest because of their unparalleled potential to produce analgesia. More recently, these receptors have been explored as targets in the treatment of drug and alcohol abuse and mood disorders.[21]

The opioid receptors are found in various tissues including the brain, nervous system and intestinal tract. Their endogenous ligands are peptides that are distributed throughout the CNS and peripheral tissues and have selectivities for the various opioid receptors. There are many opioid peptides and active peptide fragments; the ones that have received considerable attention include the endorphins, dynorphins, and enkephalins.[22] For an overview of common opioid peptides and example structures, see Table 1.2.

Table 1.2: Opioid receptors, their mammalian endogenous ligands, and example sequences

Receptor	Endogenous Ligands	Example Sequence
MOP	β-Endorphins	YGGFMTSEKSQTPLVTLFKNAIIKNAYKKGE[a]
	Endomorphins	YPWF-NH_2[b]
KOP	Dynorphins	YGGFLRRIRPKLKWDNQ[c]
DOP	Enkephalins	YGGFL[d]
NOP	Nociceptin	FGGFTGARKSARKLANQ

[a]β-Endorphin, [b]Endomorphin-1 [c]Dynorphin A, [d]Leu-Enkephalin

The dynorphins are derived from post-translational processing of prodynorphin, an inactive precursor protein.[23] These peptides have sequences at the N- terminus referred to as the "message" that convey agonist activity at opioid receptors as well as sequences at the C-terminus called the "address" which enhance affinity for their target receptors.[24] They preferentially bind to and activate the kappa opioid receptor (KOPr), causing downstream signaling that can occur through the inhibition of adenylate cyclase activity or activation of mitogen activated protein kinase.[25] In addition to analgesia, KOPr activation has been known to play a role in neurological stress effects,[25] which make both KOPr agonists and antagonists targets of interest for the treatment of depression and stress-induced reinstatement of drug and alcohol abuse.

While KOPr agonists have long been explored as therapies for pain management, this class of molecules have differing levels of effectiveness in different models of pain.[26] Agonists appear to be more effective at blocking responses against mechanical stimuli and chemical irritants than against thermal stimuli. KOPr agonists have also shown potent activity in models of visceral pain, which appears to be mediated peripherally.[27] KOPr activation has the benefit of producing anti-inflammatory effects as well as analgesia, increasing the therapeutic potential of KOPr agonists.[28] These ligands have the potential to mediate analgesia both through the central nervous system (CNS) and peripherally.[29]

KOPr agonists have several potential advantages over currently available mu opioid receptor (MOPr) agonists, such as morphine and fentanyl, approved for the treatment of pain. Notably, KOPr agonists generally show lower addictive liability compared to MOPr agonists. They commonly lack reinforcing effects and have been reported to reduce tolerance to morphine.[30] As the abuse of prescription drugs extracts increasing costs on the US healthcare system, these are attractive characteristics for potential analgesics. Additionally, KOPr activation does not cause the respiratory depression associated with MOPr activation.[31] However, some of effects of central KOPr agonism are undesirable, particularly dysphoria and sedation.[32, 33] This side effect profile has limited the development of centrally active KOPr agonists, although peripherally acting agonists are still of considerable interest.[29]

There are other applications of KOPr agonists in addition to analgesia. KOPr activation has been shown to block the reinforcing effects of alcohol and cocaine. The KOPr-selective agonist U50,488 (Figure 1.1) has been shown to attenuate both ethanol[34] and cocaine consumption.[35] It was also effective in suppressing conditioning by both substances of abuse in condition of place preference (CPP) models.[36, 37] However, it should be noted that U50,488 was observed to potentiate cocaine CPP in a time-dependent manner.[37] Several studies have suggested that repeated administration of KOPr agonists may increase cocaine-seeking behavior by increasing extracellular dopamine levels[38] and enhance dopamine signaling.[39, 40] This time-dependent phenomenon is still being studied, but results suggest that KOPr agonists may be more effective as acute interventions for cocaine addiction rather than as long term treatments.[41]

KOPr antagonists also have potential for clinical development.[42] While selective KOPr agonists can produce dysphoria, antagonists have shown potential in forced swim studies as antidepressants.[43] In fact, the KOPr selective antagonist LY2456302 (Figure 1.1) is in clinical development as a treatment for depression.[44, 45] There is mounting evidence that selective KOPr

antagonists may be effective treatments for stress and anxiety.[25] KOPr antagonists have also shown potential to treat addictions, but at different stages in addiction than agonists. KOPr antagonists have been shown to prevent cocaine self-administration[46] as well as stress-induced reinstatement of cocaine-seeking behavior.[47-49] They also reduced operant self-administration in rats selectively bred for alcohol preference.[45, 50, 51]

It should be noted here that buprenorphine, a MOPr partial agonist, KOPr antagonist/weak partial agonist, has been combined with various MOPr antagonists to act as a functional KOPr antagonist and is being studied for the treatment of cocaine and opioid addiction.[52, 53] Additionally, the combination of buprenorphine and samidorphan (a naltrexone derivative) designated ALKS 5461 is in clinical development for the treatment of major depression.[54]

KOPr ligands are being explored for many other therapeutic indications, including nicotine addiction.[21] Thus, data suggest that KOPr agonists and antagonists have significant potential for pharmaceutical development. While some indications such as peripheral pain management could be attained with peripherally restricted KOPr ligands, central activity is needed to influence stress, mood, and behavior.

Both peptide and small-molecule ligands for the KOPr have been pursued for clinical development, but no KOPr selective ligand has yet been approved. Small molecule KOPr agonists include the peripherally selective compounds fedotozine and asimadoline (Figure 1.1), which were not effective in clinical trials,[55, 56] and centrally acting compounds U50,488, which is primarily used as a pharmacological tool, and salvinorin A (Figure 1.1).[57] Clinical development of classical small-molecule KOPr antagonists such as JDTic (Figure 1.1) could be hampered by their exceptionally long durations, lasting weeks to more than a month.[58] While shorter-acting small-molecules antagonists have recently been developed, the mechanism of the long half-lives of prototypical KOPr antagonists is still undergoing study.[42] There is evidence that these half-lives

may be due to prolonged residencies of long-acting antagonists in the brain.[59] However, other studies suggest that the long durations are due to activation of c-Jun N-terminal kinase (JNK) phosphorylation by long-acting KOPr antagonists such as JDTic and nor-binaltorphimine (norBNI) rather than by the persistence of these ligands at the receptor. Some long-acting KOPr antagonists such as JDTic and norBNI seem to stimulate JNK1 phosphorylation through KOPr while some short-acting antagonists do not,[60, 61] and the durations of action of the long lasting antagonists were shortened after pretreatment with either readily reversible opioid antagonists or the JNK inhibitor SP600125.

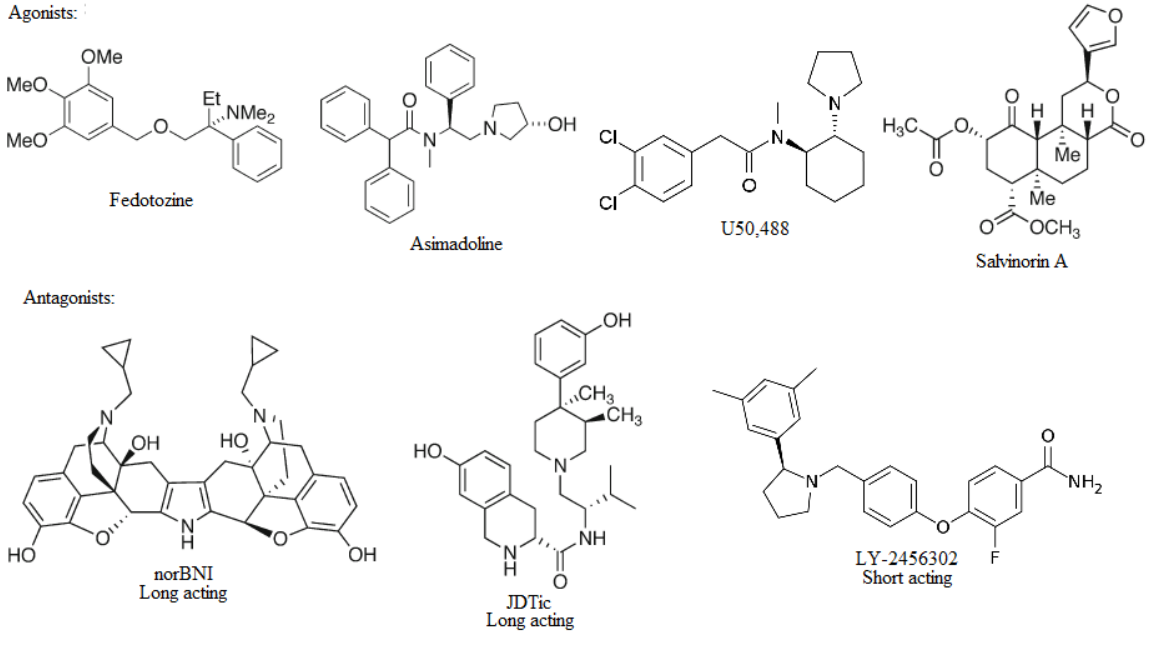

Figure 1.1: Examples of small molecule KOPr ligands

1.3 Peptide ligands of the kappa opioid receptor

Peptide KOPr agonists and antagonists have been shown to exhibit similar pharmacodynamic properties to their small-molecule counterparts, but with different metabolic and distribution properties. For the purpose of this discussion, we will focus on peptides with *in vivo* activity. Many reported KOPr selective peptide agonists are analogs of dynorphin A (Dyn A) (1-13).[62] While this peptide is metabolically unstable, many modifications can be made to increase its half-life *in vivo*, including the incorporation of a reduced peptide bond,[63] a D amino acid,[64] or an N-MeTyr and/or C-terminal amide at the N- and C-termini, respectively.[65] Analogs with modifications at the termini enhanced morphine analgesia *in vivo* in morphine-tolerant rats for 3-4 h after either intravenous or pulmonary delivery.[66] The peptide SK-9709 ([D-Ala^{2}Arg$^6\Psi$(CH_2NH)Arg^7]Dyn A-(1-8) amide) (Figure 1.2), which contains a reduced amide bond between Arg^6 and Arg^7, has also shown antinoniceptive activity *in vivo*.[63] SK-9709 shows equal or greater activity than U50,488 after systemic (subcutaneous, s.c.) in mice in both the acetic acid stretching and hot-plate assays. While *in vitro* data indicates that SK-9709 has a 15-fold higher selectivity for KOPr over MOPr, its *in vivo* opioid agonist activity seems to be mediated by both receptors, as both norBNI, administered intrathecal (i.t.) and the MOPr antagonist β-FNA, administered intracerebroventricular (i.c.v.), reversed the antinociceptive effects of SK-9709.

Agonists

[NMeTyr1]Dyn A-(1-13)NH2	MeTyr-Gly-Gly-Phe-Leu-Arg-Arg-Ile-Arg-Pro-Lys-Leu-Lys-NH_2
E-2078	MeTyr-Gly-Gly-Phe-Leu-Arg-NMeArg-D-Leu-NHEt
SK-9709	MeTyr-D-Ala-Gly-Phe-Leu-Arg$\psi(CH_2NH)$Arg-NH_2
FE200665	H-D-Phe-D-Phe-D-Nle-D-Arg-NH-4-picoly

Antagonists

JVA-901	Ac-Tyr-Lys-Trp-Trp-Leu-Arg-Arg-D-Ala-Arg-Pro-Lys-NH_2
Arodyn	Ac-Phe-Phe-Phe-Arg-Leu-Arg-Arg-D-Ala-Arg-Pro-Lys-NH_2
Zyklophin	Bz-Tyr-Gly-Gly-Phe-D-Asp-Arg-Arg-Dap-Arg-Pro-Lys-NH_2
Dynantin	(2*S*)-Mdp-Gly-Gly-Phe-Leu-Arg-Arg-Ile-Arg-Pro-LysNH_2
[Pro^3]-Dyn A-(1-11)NH_2	Tyr-Gly-Pro-Phe-Leu-Arg-Arg-Ile-Arg-Pro-LysNH_2

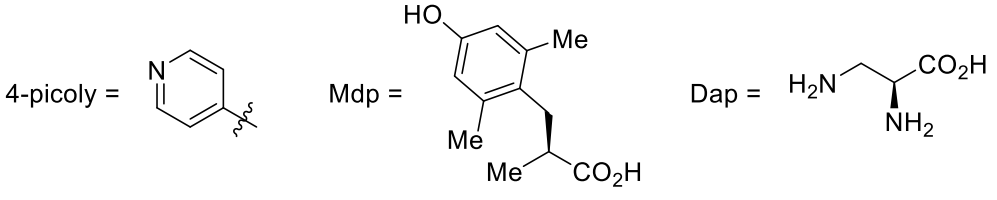

Figure 1.2: Examples of peptide KOPr ligands

The activities of peptide KOPr agonists are dependent on whether they are centrally active or peripherally selective. One Dyn A analog that can penetrate the CNS is E-2078 ([$NMeTyr^1$, $NMeArg^7$,$D\text{-}Leu^8$]Dyn A-(1-8) N-ethyl amide, Figure 1.2).[67] This peptide has been studied in rodents,[68-70] monkeys,[71-73] and humans,[74, 75] and appears to induce analgesic effects primarily through KOPr.[69] The peptide and its radiolabeled analog were detected in mice brains after a brain perfusion study[68] and monkey brains after systemic administration, respectively.[71] An *in vitro* blood-brain barrier (BBB) model using the bovine brain microvessel endothelial cell (BBMEC) model indicated that [^{125}I-Tyr]E-2078 was transported across the BBB by absorptive-mediated endocytosis.[76] In contrast, FE200665 (CR 665 or JNJ 38488502, H-D-Phe-D-Phe-D-Nle-D-Arg-NH-4-picoly, Figure 1.2,) appears to be peripherally selective,[77] thereby limiting centrally mediated side effects such as sedation or locomotor impairment. This compound is currently under

clinical development by Johnson and Johnson,[78] and while FE200665 is not itself orally bioavailable, its analogs have yielded several orally bioavailable leads.[79]

Peptides have shown promise as KOPr antagonists as well. Dyn A analogs with antagonistic activity generally have modifications in the N-terminal Tyr-Gly-Gly-Phe "message" sequence[80] and include peptides without a basic amine terminus,[81, 82] Pro^3 derivatives,[83, 84] and cyclic derivatives.[85, 86] Arodyn (Figure 1.2) is a linear peptide that has *in vivo* KOPr antagonist activity following i.c.v. administration in mice, blocking the antinociceptive effects of U50,488 in the 55 °C warm water tail withdrawal assay.[48] It is also effective in blocking stress-induced reinstatement of cocaine-seeking behavior in a CPP model in mice, but is rapidly metabolized in blood,[87] limiting systemic administration. A peptide with greater metabolic stability is zyklophin (Figure 1.2), an analog that is cyclized through two of its residues in the "address" sequence.[86] Not only does it have peripheral antagonist activity after systemic administration, [88] but it is also able to block the antinociceptive activity of centrally administered U50,488, suggesting that is able to penetrate the BBB. Further, these peptide KOPr antagonists show more finite duration of action than classical small-molecule antagonists, for example zyklophin[88] exhibits a duration of action of about 12 h rather than the weeks observed for norBNI and JDTic.[41] These *in vivo* studies of these peptides demonstrate the pharmacological potential of peptide ligands of KOPr.

1.4 CJ-15,208 and [D-Trp]CJ-15,208: Pharmacodynamics, pharmacokinetics, and structure-activity relationships

The macrocyclic peptide natural product CJ-15,208 (*cyclic*[Trp-Phe-D-Pro-Phe], Figure 1.3) was isolated from a fermentation broth of *Ctenomyces serratus* ATCC15502.[89] It was reported to bind to KOPr with modest affinity and selectivity and antagonize a KOR agonist *in vitro*. Because the stereochemistry of the tryptophan residue in the natural product was not known, the

Aldrich research group optimized the cyclization conditions and synthesized both the L-Trp and D-Trp isomers for testing.[90, 91] While the optical rotation of only the L-Trp isomer was consistent with the natural product, both isomers exhibited similar nanomolar affinity for KOPr. Both isomers showed *in vitro* KOPr antagonism in a guanosine-5'-(3-thiotriphosphate) (GTPγS) binding assay,[92] but have displayed surprisingly different activity profiles *in vivo*.[92]

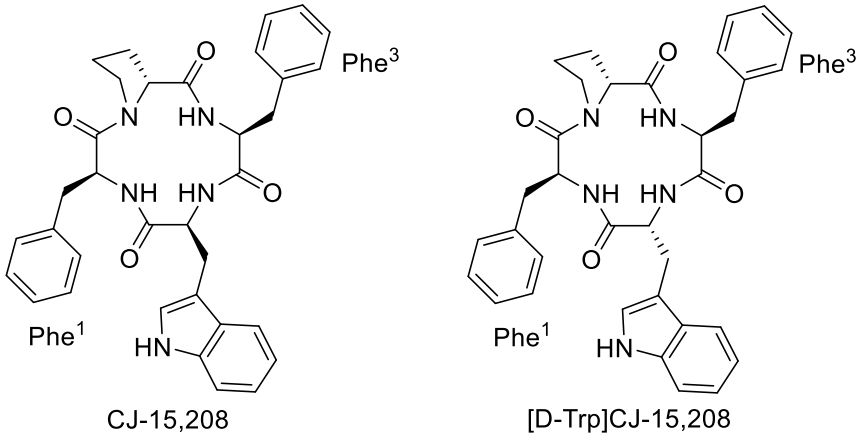

Figure 1.3: CJ-15,208 and [D-Trp]CJ-15,208

The D-Trp isomer (Figure 1.3) has shown predominantly KOPr antagonist activity *in vivo* with only minimal agonist activity at high doses.[49, 92] It exhibits short-acting antagonist activity, and is able to block the antinociceptive activity of U50,488 administered systemically (intraperitoneal, i.p.) after various routes of administration: central (3 nmol i.c.v., <18 h duration of action), peripheral (10 mg/kg s.c., <18 h duration of action), and oral (10 mg/kg p.o., <12 h duration of action).[49, 92] Further, it blocks the antinociceptive activity of U50,488 administered centrally (i.c.v.) after oral administration (30 mg/kg p.o., <6 h duration of action), indicating its ability to cross the BBB with no impairment of locomotor activity. The CNS penetration of orally administered [D-Trp]CJ-15,208 was verified by detection of this peptide in the brain by liquid

chromatography tandem mass spectrometry (LC-MS/MS). Additionally, orally administered [D-Trp]CJ-15,208 prevented stress-, but not cocaine-induced, reinstatement of extinguished cocaine-seeking behavior in mice in a CPP assay, consistent with its KOPr antagonist activity.

The L-Trp isomer (the natural product) has shown both agonist (antinociceptive) activity and short-acting KOPr antagonist activity *in vivo*. It exhibits short-acting antagonist activity and is able to block the antinociceptive activity of U50,488 administered systemically (i.p.) after central (3 nmol i.c.v., <18 h duration of action) and oral administration (10 mg/kg p.o., <12 h duration of action).[92, 93] CJ-15,208 also shows opioid agonist activity mediated by both KOPr and MOPr after oral administration (60 mg/kg p.o., <3 h duration) without affecting locomotor activity. The peptide shows CNS activity after oral administration, antagonizing the antinociceptive activity of U50,488 administered centrally (i.c.v.). Interestingly, orally administered CJ-15,208 is able to prevent both cocaine- and stress-induced reinstatement of extinguished cocaine-seeking behavior in the CPP assay in a time- and dose-dependent manner.

These peptides have shown unusual structure-activity relationships. While small modifications can have radical effects on activity profiles, some analogs with significant substitutions retain activity. Alanine scan analogs of both isomers were generated and tested *in vivo* and *in vitro* to determine the residues involved in mediating activity. Each of the alanine analogs of CJ-15,208 retained opioid agonist and KOPr antagonist activity of the parent compound after i.c.v. administration in an antinociceptive assay, but the opioid agonism of the analogs was predominately mediated by MOPr.[94] The Ala^3 analog showed the most potent agonist activity. The Ala^3 and Ala^1 analogs had antagonist activity comparable to the parent compound.

In contrast to the current parent peptide, alanine substitution for any residues of [D-Trp]CJ-15,208 resulted in antinociceptive (opioid agonist) activity in this assay following i.c.v. administration.[95] The *in vivo* KOPr antagonist activity of the parent peptide was retained in all

analogs except the D-NMeAla^2, suggesting that the D-Pro residue is important for KOPr antagonist activity. Further, analogs with alanine substituted for the D-Trp or Phe^1 positions prevented stress-induced, but not cocaine-primed, reinstatement of cocaine CPP after i.c.v. pretreatment. It should also be noted that the alanine scan analogs of the two isomers exhibited similar *in vitro* profiles that were not indicative of their *in vivo* activities.

The Dolle laboratory synthesized a series of [D-Trp]CJ-15,208 analogs and evaluated their binding and selectivity exclusively *in vitro*.[96] This study indicated that linear analogs of the cyclic peptides had little appreciable affinity for the opioid receptors. In a series of [D-Trp]CJ-15,208 analogs with substitutions on either phenylalanine residue, peptides containing tyrosine substituted for phenylalanine displayed a substantial loss in KOPr affinity. Analogs incorporating m-Tyr residues retained higher KOPr affinity, but lost selectivity over MOPr. Substitution at the 4' position on either Phe residue with either a methoxy or fluorine resulted in modest affinity at KOPr.

These macrocyclic peptides also have acceptable pharmacokinetic properties in *in vitro* models. CJ-15,208 and its D-Trp analog show remarkable stability in plasma and whole blood for at least 20 h,[97] indicating resistance to proteases. However, studies in liver microsomes indicate susceptibility to oxidation, presumably through cytochrome p450 (CYP-P450) enzymes, resulting in relatively short half-lives for both CJ-15,208 (60 min) and especially [D-Trp]CJ-15,208 (12 min). Other cyclic peptides, including cyclic prodrugs of [D-Ala^2, D-Leu^5]encephalin (DADLE), a pentapeptide opioid agonist primarily acting through delta opioid receptor (DOPr), have been shown to be unstable in rat and guinea pig liver microsomes, showing nearly complete degradation after 15 min.[98] Interestingly, studies of DADLE and its capped and cyclic analogs indicate that the cyclized peptides were less susceptible to hydrolytic metabolism, possibly due to high protein binding,[99] but more susceptible to metabolism by CYP P450 enzymes than their linear

counterparts.[98] As CYP P450 enzymes are present both in liver and brain tissue,[100, 101] susceptibility to oxidative metabolism can affect central activity.

1.5 Overview of the blood-brain barrier

While peripherally selective KOPr agonists can be used in the treatment of some forms of pain, central activity is required for the treatment of drug and alcohol addiction. However, few CNS drug candidates make it to the market. About 10% of all therapeutic compounds that enter phase I clinical trials become marketed drugs compared to only 3-5% of centrally acting agents.[102] Part of the reason oral CNS agents often fail in clinical trials is because of the BBB. The BBB is a complex cellular construct that separates brain matter from the systemic circulation. It acts as a physical barrier to protect the brain's homeostasis and keep toxins out of the CNS, and represents a serious challenge for centrally acting drugs. Approximately 98% of small molecule drugs and almost all large molecule neurotherapeutics cannot cross the BBB.[103] This barrier has eliminated many neuroactive peptides and biologics with promising activity from clinical use.[8]

The BBB has a diverse set of components that can either hinder or facilitate drug transport into the CNS. The BBB is involved is some metabolism, mostly carried out by aminopeptidases, endopeptidases, and cholinesterases.[104] Drugs can also be metabolized in the brain by CYP-P450s.[105] Paracellular transport of hydrophilic drugs between the brain endothelial cells is typically prevented by tight junctions and adherens junctions between the cells.[106] Tight junctions are formed by a network of intercellular proteins, including occludin, zonula occludens, and claudins, between adjacent cells to form a continuous barrier between the cells.[106] Adherens junctions from a slightly more penetrable barrier than tight junctions, and are formed between cells through the integral membrane proteins VE-cadherin and PECAM-1. The actin cytoskeleton, to which many

of these integral membrane proteins are anchored, has also been shown to play a role in the integrity of these junctions.[107]

Small, relatively lipophilic molecules are likely to passively diffuse across the BBB,[108] which is the most common means of transport into the CNS of centrally acting therapeutics approved by the FDA.[109] Passive diffusion is a process in which the aqueous solvent shell around the compound is dissipated and it dissolves into a lipid bilayer; another aqueous solvent shell must form around the compound after passing through to the other side of the membrane. Because of the differences between the intestinal barrier and the BBB, Lipinski's rule of 5 has been modified to predict CNS penetration. To optimize passive diffusion into the brain, small molecule drugs should meet the following criteria: Molecular weight ≤400, LogP ≤5, hydrogen bond donors ≤3, and hydrogen bond acceptors ≤7.[110] While most peptides do not fall within these ranges, these rule were not constructed around polypeptide CNS permeability.

While it is possible for polypeptides with a molecular weight up to 4.1 kDa to passively diffuse across the BBB,[111] many researchers are exploring strategies to deliver polypeptides into the brain that take advantage of the BBB's active and facilitated transporters. Receptor-mediated transport is responsible for transporting larger peptides and proteins like transferrin and insulin across the BBB.[112] Opioid peptides have also been shown to be actively transported via endocytosis.[76]

Passive transcellular transport of some drugs across the BBB can be hindered by efflux proteins. Efflux proteins are integral membrane proteins that are highly expressed in the BBB and actively transport a broad range of compounds, particularly potentially harmful chemical entities, out of the CNS.[113] These effective proteins include ATP-binding cassette (ABC) transporters, such as P-glycoprotein (P-gp), and the breast cancer resistant protein (BCRP).[114] P-gp is responsible for the ATP-dependent efflux of many lipophilic, amphipathic, and cationic drugs, and is the most

commonly examined efflux protein in drug design. Inhibitors of P-gp include verapamil, CSA and quinidine. Several cyclic peptides have been shown to be effluxed by both P-gp and BCRP,[115] limiting their central exposure. Conversely, P-gp efflux has been used as a strategy to restrict therapeutics to the periphery. For example, P-gp has reduced the negative side effects caused by central exposure of both CSA[116] and small molecule KOPr agonists.[117]

1.6 Assays for transport

Passive diffusion assays are the fastest and most cost efficient methods for assessing transport early in compound design.[102] These include immobilized artificial membrane (IAM) columns, the parallel artificial membrane permeability assay (PAMPA), and PAMPA-BBB. IAM columns are made up of phospholipids bonded to the silica gel. Liquid chromatography using these columns gives a retention time that has been shown to be a better predictor than logP for CNS penetration.[118] However, this method does not give a permeability constant. PAMPA allows for the measurement of passive diffusion across an artificial bilayer membrane made of phospholipids. This model can be modified to better mimic the BBB by using porcine polar brain lipid extracts to form the membrane, in which case the assay is termed PAMPA-BBB.[119] The PAMPA assays and the IAM column are high throughput and very reproducible, but they do not model efflux or facilitated transport.

Compound transport can also be measured in assays that are designed to mimic the BBB. Monolayers of primary cultures of brain endothelial cells, such as BBMEC, have shown utility in studying peptides.[120, 121] However, formation of tight junctions can be variable and must be closely monitored to maintain reproducibility. A new assay attempts to overcome these difficulties by using a stem-cell based model of the BBB.[122] Lippmann *et al*. co-cultured both human embryonic stem cells and human induced pluripotent stem cells with astrocytes to induce BBB characteristics.

The stem cells were observed to form tight junctions and express sufficient amounts of transporters to serve as a representative model of the BBB.

Other *in vitro* models can be used to model compounds' potential penetration into the CNS.[102] The Caco-2 and Madin-Darby canine kidney (MDCK) cell lines are accepted *in vitro* models of the intestinal barrier. Despite the fundamental differences between these cell lines and those found in the BBB, they can be used to predict whether candidates will be substrates of efflux proteins that are found in the BBB.[13] Caco-2 cells express sufficient levels of efflux proteins for study, and efflux protein genes, such as the P-gp gene MDR1, can be transfected into MDCK cells. Since both cell lines are polar, the ratio of compound transported from the apical (A) to the basolateral (B) side compared to from B to A can be used as an indication of whether the compound is a substrate for efflux proteins. The exact proteins involved in efflux can be deduced by performing efflux inhibitor studies.

Both *in vivo* and *in vitro* models of the BBB have been used to study opioid peptides with *in vivo* activity. A number of opioid peptides have been studied for BBB permeability. Enkephalin analogs with permeability and activity in the CNS have been designed and tested. Several strategies were employed for improving their transport across the BBB. Glycosylation on the cyclic opioid peptide *cyclo*[D-Cys^{2,5},Ser^{6},Gly^{7}]enkephalin with various sugar moieties improved *in situ* brain uptake in rats by up to 98%.[123] The glycosylation was shown to significantly lower LogP and slightly decreased peptide binding to bovine serum albumin. In other cases, increasing the LogP through the introduction of halogens improved peptide transport.[124] For example, the peptide biphalin ([Tyr-D-Ala-Gly-Phe-NH]$_2$), a dimeric enkephalin analog with activity at both the MOPr and DOPr,[125] showed both passive diffusion and active transport via the large neutral amino acid carrier in in situ brain perfusion studies.[126] Halogenated biphalin analogs were screened

in *in vitro* and *in situ* models of the BBB, and a chlorohalogenated analog showed both increased uptake and biological stability.[127]

Facilitated transport was also observed in studies of opioid peptides. The peptide [D-penicillamine[2,5]]enkephalin (DPDPE) is a cyclic DOPr agonist that displayed passive diffusion in a primary endothelial cell culture model of the BBB, but its transport greatly increases in the presence of insulin both *in vitro* and *in situ*.[126, 128] It was postulated that its transport might be augmented by the transcytosis induced by insulin's receptor-mediated transport across the BBB.

Several other cyclic peptides have shown permeability in models of the BBB. The Borchardt lab produced a series of cyclic prodrugs of the peptide DADLE (H-Tyr-D-Ala-Gly-Phe-D-Leu-OH), an enkephalin analog, and studied their transport across monolayers Caco-2[129-131] and MDCK-MDR1 cells.[115] Many of the cyclic peptides had improved permeability compared to the parent compound,[130, 131] but the transport of some of the analogs appeared to be limited by efflux,[129] especially by P-gp.[115] Studies in Caco-2 monolayers suggested that CJ-15,208 was an efflux substrate,[132] but the efflux proteins involved have not been identified.

1.7 Importance of current work

While drug addiction continues to represent a burden on the U.S. economy, there are currently no FDA approved pharmaceutical treatments for cocaine addiction, and the most commonly prescribed analgesics have agonist activity at MOPr, which is associated with addictive liability. KOPr agonists have potential as non-addictive analgesics, and both KOPr agonists and antagonists have potential in the treatment of cocaine addiction. While the clinical applications of many small-molecule KOPr ligands have been limited by side effects, peptide ligands could be promising leads, however their pharmacokinetic properties must be assessed, and possibly modified by incorporating structural changes.

The experiments in mice discussed above indicate that CJ-15,208 has antinociceptive activity and can block cocaine-induced reinstatement of cocaine CPP, and that both it and [D-Trp]CJ-15,208 can prevent stress-induced reinstatement of cocaine CPP. Further, these peptides are orally bioavailable, cross the BBB, and do not induce side effects such as sedation. However, large doses of these peptides are required for oral activity, and bioavailability may be limited by rapid oxidative metabolism and/or efflux at the intestinal and/or blood-brain barriers.

In this study, CJ-15,208 and [D-Trp]CJ-15,208 are evaluated in MDCK cells, both in wild type (WT) cells and cells transfected with the P-gp gene MDR1, to determine their transport and interactions with the efflux protein P-gp. Identifying interactions with specific efflux proteins can aid in the design of future analogs. We also synthesized deuterated probes to examine oxidative metabolism patterns of CJ-15,208 and [D-Trp]CJ-15,208 and the effects of structure modification on opioid activity. This information could aid in the design of metabolism-resistant analogs. Analogs of CJ-15,208 and [D-Trp]CJ-15,208 incorporating fluorine, hydroxyl, and methoxy groups into their aromatic residues were synthesized to potentially improve absorption and distribution properties. These compounds are being screened for *in vivo* activity.

1.8 References

1. Penrod, N. M.; Cowper-Sal-lari, R.; Moore, J. H. Systems genetics for drug target discovery. *Trends Pharmacol. Sci.* **2011,** 32, 623-630.

2. Graul, A. I.; Lupone, B.; Cruces, E.; Stringer, M. 2012 in review - part I: the year's new drugs & biologics. *Drugs Today (Barc)* **2013,** 49, 33-68.

3. Craik, D. J.; Fairlie, D. P.; Liras, S.; Price, D. The future of peptide-based drugs. *Chem Biol Drug Des* **2013,** 81, 136-47.

4. McGonigle, P. Peptide therapeutics for CNS indications. *Biochem Pharmacol* **2012,** 83, 559-66.

5. Grant, M.; Leone-Bay, A. Peptide therapeutics: it's all in the delivery. *Ther Deliv* **2012,** 3, 981-96.

6. Lipinski, C. A. Drug-like properties and the causes of poor solubility and poor permeability. *J Pharmacol Toxicol Methods* **2000,** 44, 235-49.

7. Veber, D. F.; Johnson, S. R.; Cheng, H.-Y.; Smith, B. R.; Ward, K. W.; Kopple, K. D. Molecular properties that influence the oral bioavailability of drug candidates. *J Med Chem* **2002,** 45, 2615-2623.

8. Pajouhesh, H.; Lenz, G. R. Medicinal chemical properties of successful central nervous system drugs. *NeuroRx* **2005,** 2, 541-553.

9. Vlieghe, P.; Lisowski, V.; Martinez, J.; Khrestchatisky, M. Synthetic therapeutic peptides: science and market. *Drug Discov Today* **2010,** 15, 40-56.

10. White, T. R.; Renzelman, C. M.; Rand, A. C.; Rezai, T.; McEwen, C. M.; Gelev, V. M.; Turner, R. A.; Linington, R. G.; Leung, S. S.; Kalgutkar, A. S.; Bauman, J. N.; Zhang, Y.; Liras, S.; Price, D. A.; Mathiowetz, A. M.; Jacobson, M. P.; Lokey, R. S. On-resin N-methylation of cyclic peptides for discovery of orally bioavailable scaffolds. *Nat Chem Biol* **2011,** 7, 810-7.

11. Saeki, T.; Ueda, K.; Tanigawara, Y.; Hori, R.; Komano, T. Human P-glycoprotein transports cyclosporin A and FK506. *J Biol Chem* **1993,** 268, 6077-80.

12. von Richter, O.; Glavinas, H.; Krajcsi, P.; Liehner, S.; Siewert, B.; Zech, K. A novel screening strategy to identify ABCB1 substrates and inhibitors. *Naunyn Schmiedebergs Arch Pharmacol* **2009,** 379, 11-26.

13. Garberg, P.; Ball, M.; Borg, N.; Cecchelli, R.; Fenart, L.; Hurst, R. D.; Lindmark, T.; Mabondzo, A.; Nilsson, J. E.; Raub, T. J.; Stanimirovic, D.; Terasaki, T.; Oberg, J. O.; Osterberg, T. In vitro models for the blood-brain barrier. *Toxicol In Vitro* **2005,** 19, 299-334.

14. Avdeef, A. How well can the Caco-2/Madin−Darby canine kidney models predict effective human jejunal permeability? *J Med Chem* **2010,** 53, 3566-3584.

15. Okumu, F. W.; Pauletti, G. M.; Vander Velde, D. G.; Siahaan, T. J.; Borchardt, R. T. Effect of restricted conformational flexibility on the permeation of model hexapeptides across Caco-2 cell monolayers. *Pharm Res* **1997,** 14, 169-75.

16. Rezai, T.; Bock, J. E.; Zhou, M. V.; Kalyanaraman, C.; Lokey, R. S.; Jacobson, M. P. Conformational flexibility, internal hydrogen bonding, and passive membrane permeability: successful in silico prediction of the relative permeabilities of cyclic peptides. *J Am Chem Soc* **2006,** 128, 14073-80.

17. Beck, J. G.; Chatterjee, J.; Laufer, B.; Kiran, M. U.; Frank, A. O.; Neubauer, S.; Ovadia, O.; Greenberg, S.; Gilon, C.; Hoffman, A.; Kessler, H. Intestinal permeability of cyclic peptides: common key backbone motifs identified. *J Am Chem Soc* **2012,** 134, 12125-33.

18. Ovadia, O.; Greenberg, S.; Chatterjee, J.; Laufer, B.; Opperer, F.; Kessler, H.; Gilon, C.; Hoffman, A. The effect of multiple N-methylation on intestinal permeability of cyclic hexapeptides. *Mol Pharm* **2011,** 8, 479-487.

19. Brunton, L.; Chabner, B.; Knollman, B. Chapter 18: Opioids, Analgesia, and Pain Management. In *Goodman and Gilman's The Pharmacological Basis of Therapeutics (12th ed.)*, McGraw-Hill Professional: New York, USA, 2010.

20. Mollereau, C.; Parmentier, M.; Mailleux, P.; Butour, J. L.; Moisand, C.; Chalon, P.; Caput, D.; Vassart, G.; Meunier, J. C. ORL1, a novel member of the opioid receptor family. Cloning, functional expression and localization. *FEBS Lett* **1994,** 341, 33-8.

21. Feng, Y.; He, X.; Yang, Y.; Chao, D.; Lazarus, L. H.; Xia, Y. Current research on opioid receptor function. *Curr Drug Targets* **2012,** 13, 230-46.

22. Kosterlitz, H. W. The Wellcome Foundation lecture, 1982. Opioid peptides and their receptors. *Proc R Soc Lond B Biol Sci* **1985,** 225, 27-40.

23. Schwarzer, C. 30 years of dynorphins--new insights on their functions in neuropsychiatric diseases. *Pharmacol Ther* **2009,** 123, 353-70.

24. Chavkin, C.; Goldstein, A. Specific receptor for the opioid peptide dynorphin: structure--activity relationships. *Proc Natl Acad Sci U S A* **1981,** 78, 6543-6547.

25. Van't Veer, A.; Carlezon, W. A., Jr. Role of kappa-opioid receptors in stress and anxiety-related behavior. *Psychopharmacology (Berl)* **2013,** 229, 435-52.

26. Millan, M. J. Kappa-opioid receptors and analgesia. *Trends Pharmacol Sci* **1990,** 11, 70-6.

27. Riviere, P. J. Peripheral kappa-opioid agonists for visceral pain. *Br J Pharmacol* **2004,** 141, 1331-4.

28. Walker, J. S. Anti-inflammatory effects of opioids. *Adv Exp Med Biol* **2003,** 521, 148-60.

29. DeHaven-Hudkins, D. L.; Dolle, R. E. Peripherally restricted opioid agonists as novel analgesic agents. *Curr Pharm Des* **2004,** 10, 743-57.

30. Pan, Z. Z. mu-Opposing actions of the kappa-opioid receptor. *Trends Pharmacol Sci* **1998,** 19, 94-8.

31. Mutolo, D.; Bongianni, F.; Einum, J.; Dubuc, R.; Pantaleo, T. Opioid-induced depression in the lamprey respiratory network. *Neuroscience* **2007,** 150, 720-9.

32. Pfeiffer, A.; Brantl, V.; Herz, A.; Emrich, H. M. Psychotomimesis mediated by kappa opiate receptors. *Science* **1986,** 233, 774-6.

33. Mello, N. K.; Negus, S. S. Interactions between kappa opioid agonists and cocaine. Preclinical studies. *Ann N Y Acad Sci* **2000,** 909, 104-32.

34. Lindholm, S.; Werme, M.; Brene, S.; Franck, J. The selective kappa-opioid receptor agonist U50,488H attenuates voluntary ethanol intake in the rat. *Behav Brain Res* **2001,** 120, 137-46.

35. Negus, S. S. Effects of the kappa opioid agonist U50,488 and the kappa opioid antagonist nor-binaltorphimine on choice between cocaine and food in rhesus monkeys. *Psychopharmacology (Berl)* **2004,** 176, 204-13.

36. Logrip, M. L.; Janak, P. H.; Ron, D. Blockade of ethanol reward by the kappa opioid receptor agonist U50,488H. *Alcohol* **2009,** 43, 359-65.

37. McLaughlin, J. P.; Land, B. B.; Li, S.; Pintar, J. E.; Chavkin, C. Prior activation of kappa opioid receptors by U50,488 mimics repeated forced swim stress to potentiate cocaine place preference conditioning. *Neuropsychopharmacol* **2006,** 31, 787-94.

38. Fuentealba, J. A.; Gysling, K.; Magendzo, K.; Andres, M. E. Repeated administration of the selective kappa-opioid receptor agonist U-69593 increases stimulated dopamine extracellular levels in the rat nucleus accumbens. *J Neurosci Res* **2006,** 84, 450-9.

39. Heidbreder, C. A.; Schenk, S.; Partridge, B.; Shippenberg, T. S. Increased responsiveness of mesolimbic and mesostriatal dopamine neurons to cocaine following repeated administration of a selective kappa-opioid receptor agonist. *Synapse* **1998,** 30, 255-62.

40. Thompson, A. C.; Zapata, A.; Justice, J. B., Jr.; Vaughan, R. A.; Sharpe, L. G.; Shippenberg, T. S. Kappa-opioid receptor activation modifies dopamine uptake in the nucleus accumbens and opposes the effects of cocaine. *J Neurosci* **2000,** 20, 9333-40.

41. Aldrich, J. V.; McLaughlin, J. P. Peptide kappa opioid receptor ligands: potential for drug development. *AAPS J* **2009,** 11, 312-22.

42. Carroll, F. I.; Carlezon, W. A. Development of κ opioid receptor antagonists. *J Med Chem* **2013,** 56, 2178-2195.

43. Mague, S. D.; Pliakas, A. M.; Todtenkopf, M. S.; Tomasiewicz, H. C.; Zhang, Y.; Stevens, W. C., Jr.; Jones, R. M.; Portoghese, P. S.; Carlezon, W. A., Jr. Antidepressant-like effects of κ-opioid receptor antagonists in the forced swim test in rats. *J Pharmacol Exp Ther* **2003,** 305, 323-330.

44. Zheng, M. Q.; Nabulsi, N.; Kim, S. J.; Tomasi, G.; Lin, S. F.; Mitch, C.; Quimby, S.; Barth, V.; Rash, K.; Masters, J.; Navarro, A.; Seest, E.; Morris, E. D.; Carson, R. E.; Huang, Y. Synthesis and evaluation of 11C-LY2795050 as a kappa-opioid receptor antagonist radiotracer for PET imaging. *J Nucl Med* **2013,** 54, 455-63.

45. Rorick-Kehn, L. M.; Witkin, J. M.; Statnick, M. A.; Eberle, E. L.; McKinzie, J. H.; Kahl, S. D.; Forster, B. M.; Wong, C. J.; Li, X.; Crile, R. S.; Shaw, D. B.; Sahr, A. E.; Adams, B. L.; Quimby, S. J.; Diaz, N.; Jimenez, A.; Pedregal, C.; Mitch, C. H.; Knopp, K. L.; Anderson, W. H.; Cramer, J. W.; McKinzie, D. L. LY2456302 is a novel, potent, orally-bioavailable small molecule kappa-selective antagonist with activity in animal models predictive of efficacy in mood and addictive disorders. *Neuropharmacol* **2014,** 77, 131-44.

46. Kuzmin, A. V.; Gerrits, M. A.; Van Ree, J. M. Kappa-opioid receptor blockade with nor-binaltorphimine modulates cocaine self-administration in drug-naive rats. *Eur J Pharmacol* **1998,** 358, 197-202.

47. Beardsley, P. M.; Howard, J. L.; Shelton, K. L.; Carroll, F. I. Differential effects of the novel kappa opioid receptor antagonist, JDTic, on reinstatement of cocaine-seeking induced by footshock stressors vs cocaine primes and its antidepressant-like effects in rats. *Psychopharmacology (Berl)* **2005,** 183, 118-26.

48. Carey, A. N.; Borozny, K.; Aldrich, J. V.; McLaughlin, J. P. Reinstatement of cocaine place-conditioning prevented by the peptide kappa-opioid receptor antagonist arodyn. *Eur J Pharmacol* **2007,** 569, 84-9.

49. Eans, S. O.; Ganno, M. L.; Reilley, K. J.; Patkar, K. A.; Senadheera, S. N.; Aldrich, J. V.; McLaughlin, J. P. The macrocyclic tetrapeptide [D-Trp]CJ-15,208 produces short-acting kappa opioid receptor antagonism in the CNS after oral administration. *Br J Pharmacol* **2013,** 169, 426-36.

50. Kissler, J. L.; Sirohi, S.; Reis, D. J.; Jansen, H. T.; Quock, R. M.; Smith, D. G.; Walker, B. M. The one-two punch of alcoholism: role of central amygdala dynorphins/kappa-opioid receptors. *Biol Psychiatry* **2014,** 75, 774-82.

51. Walker, B. M.; Koob, G. F. Pharmacological evidence for a motivational role of kappa-opioid systems in ethanol dependence. *Neuropsychopharmacol* **2008,** 33, 643-52.

52. Mooney, L. J.; Nielsen, S.; Saxon, A.; Hillhouse, M.; Thomas, C.; Hasson, A.; Stablein, D.; McCormack, J.; Lindblad, R.; Ling, W. Cocaine use reduction with buprenorphine (CURB): rationale, design, and methodology. *Contemp Clin Trials* **2013,** 34, 196-204.

53. Rothman, R. B.; Gorelick, D. A.; Heishman, S. J.; Eichmiller, P. R.; Hill, B. H.; Norbeck, J.; Liberto, J. G. An open-label study of a functional opioid kappa antagonist in the treatment of opioid dependence. *J Subst Abuse Treat* **2000,** 18, 277-81.

54. Ehrich, E.; Turncliff, R.; Du, Y.; Leigh-Pemberton, R.; Fernandez, E.; Jones, R.; Fava, M. Evaluation of opioid modulation in major depressive disorder. *Neuropsychopharmacol* **2015,** 40, 1448-55.

55. Lembo, A. Peripheral opioids for functional GI disease: a reappraisal. *Dig Dis* **2006,** 24, 91-8.

56. Mangel, A. W.; Hicks, G. A. Asimadoline and its potential for the treatment of diarrhea-predominant irritable bowel syndrome: a review. *Clin Exp Gastroenterol* **2012,** 5, 1-10.

57. Prisinzano, T. E.; Tidgewell, K.; Harding, W. W. Kappa opioids as potential treatments for stimulant dependence. *AAPS J* **2005,** 7, E592-9.

58. Carroll, I.; Thomas, J. B.; Dykstra, L. A.; Granger, A. L.; Allen, R. M.; Howard, J. L.; Pollard, G. T.; Aceto, M. D.; Harris, L. S. Pharmacological properties of JDTic: a novel κ-opioid receptor antagonist. *Eur J Pharmacol* **2004,** 501, 111-119.

59. Patkar, K. A.; Wu, J.; Ganno, M. L.; Singh, H. D.; Ross, N. C.; Rasakham, K.; Toll, L.; McLaughlin, J. P. Physical presence of nor-binaltorphimine in mouse brain over 21 days after a single administration corresponds to its long-lasting antagonistic effect on κ-opioid receptors. *J Pharmacol Exp Ther* **2013,** 346, 545-554.

60. Melief, E. J.; Miyatake, M.; Carroll, F. I.; Beguin, C.; Carlezon, W. A., Jr.; Cohen, B. M.; Grimwood, S.; Mitch, C. H.; Rorick-Kehn, L.; Chavkin, C. Duration of action of a broad range of selective κ-opioid receptor antagonists is positively correlated with c-Jun N-terminal kinase-1 activation. *Mol Pharmacol* **2011,** 80, 920-929.

61. Bruchas, M. R.; Yang, T.; Schreiber, S.; DeFino, M.; Kwan, S. C.; Li, S.; Chavkin, C. Long-acting κ opioid antagonists disrupt receptor signaling and produce noncompetitive effects by activating C-Jun N-terminal Kinase. *J Biol Chem* **2007,** 282, 29803-29811.

62. Naqvi, T.; Haq, W.; Mathur, K. B. Structure-activity relationship studies of dynorphin A and related peptides. *Peptides* **1998,** 19, 1277-92.

63. Hiramatsu, M.; Inoue, K.; Ambo, A.; Sasaki, Y.; Kameyama, T. Long-lasting antinociceptive effects of a novel dynorphin analogue, Tyr-D-Ala-Phe-Leu-Arg ψ (CH_2NH) Arg-NH_2, in mice. *Br J Pharmacol* **2001,** 132, 1948-56.

64. Story, S. C.; Murray, T. F.; Delander, G. E.; Aldrich, J. V. Synthesis and opioid activity of 2-substituted dynorphin A-(1-13) amide analogues. *Int J Pept Protein Res* **1992,** 40, 89-96.

65. Al-Fayoumi, S. I.; Brugos, B.; Arya, V.; Mulder, E.; Eppler, B.; Mauderli, A. P.; Hochhaus, G. Identification of stabilized dynorphin derivatives for suppressing tolerance in morphine-dependent rats. *Pharm Res* **2004,** 21, 1450-6.

66. Brugos, B.; Arya, V.; Hochhaus, G. Stabilized dynorphin derivatives for modulating antinociceptive activity in morphine tolerant rats: effect of different routes of administration. *AAPS J* **2004,** 6, e36.

67. Yoshino, H.; Nakazawa, T.; Arakawa, Y.; Kaneko, T.; Tsuchiya, Y.; Matsunaga, M.; Araki, S.; Ikeda, M.; Yamatsu, K.; Tachibana, S. Synthesis and structure-activity relationships of dynorphin A-(1-8) amide analogues. *J Med Chem* **1990,** 33, 206-12.

68. Terasaki, T.; Deguchi, Y.; Sato, H.; Hirai, K.; Tsuji, A. In vivo transport of a dynorphin-like analgesic peptide, E-2078, through the blood-brain barrier: an application of brain microdialysis. *Pharm Res* **1991,** 8, 815-20.

69. Nakazawa, T.; Furuya, Y.; Kaneko, T.; Yamatsu, K. Spinal kappa receptor-mediated analgesia of E-2078, a systemically active dynorphin analog, in mice. *J Pharmacol Exp Ther* **1991,** 256, 76-81.

70. Nakazawa, T.; Kaneko, T.; Yoshino, H.; Tachibana, S.; Goto, M.; Taki, T.; Yamatsu, K. Physical dependence liability of dynorphin A analogs in rodents. *Eur J Pharmacol* **1991,** 201, 185-9.

71. Yu, J.; Butelman, E. R.; Woods, J. H.; Chait, B. T.; Kreek, M. J. Dynorphin A (1-8) analog, E-2078, crosses the blood-brain barrier in rhesus monkeys. *J Pharmacol Exp Ther* **1997,** 282, 633-8.

72. Butelman, E. R.; Vivian, J. A.; Yu, J.; Kreek, M. J.; Woods, J. H. Systemic effects of E-2078, a stabilized dynorphin A(1-8) analog, in rhesus monkeys. *Psychopharmacology (Berl)* **1999,** 143, 190-6.

73. Butelman, E. R.; Harris, T. J.; Kreek, M. J. Effects of E-2078, a stable dynorphin A(1-8) analog, on sedation and serum prolactin levels in rhesus monkeys. *Psychopharmacology (Berl)* **1999,** 147, 73-80.

74. Ohnishi, A.; Mihara, M.; Yasuda, S.; Tomono, Y.; Hasegawa, J.; Tanaka, T. Aquaretic effect of the stable dynorphin-A analog E2078 in the human. *J Pharmacol Exp Ther* **1994,** 270, 342-7.

75. Fujimoto, K.; Momose, T. Analgesic efficacy of E2078 (dynorphin analog) in patients following abdominal surgery. *Masui* **1995,** 44, 1233-7.

76. Terasaki, T.; Hirai, K.; Sato, H.; Kang, Y. S.; Tsuji, A. Absorptive-mediated endocytosis of a dynorphin-like analgesic peptide, E-2078 into the blood-brain barrier. *J Pharmacol Exp Ther* **1989,** 251, 351-7.

77. Arendt-Nielsen, L.; Olesen, A. E.; Staahl, C.; Menzaghi, F.; Kell, S.; Wong, G. Y.; Drewes, A. M. Analgesic efficacy of peripheral kappa-opioid receptor agonist CR665 compared to oxycodone in a multi-modal, multi-tissue experimental human pain model: selective effect on visceral pain. *Anesthesiology* **2009,** 111, 616-24.

78. Olesen, A. E.; Kristensen, K.; Staahl, C.; Kell, S.; Wong, G. Y.; Arendt-Nielsen, L.; Drewes, A. M. A population pharmacokinetic and pharmacodynamic study of a peripheral kappa-opioid receptor agonist CR665 and oxycodone. *Clin Pharmacokinet* **2013,** 52, 125-37.

79. Hughes, F. M., Jr.; Shaner, B. E.; Brower, J. O.; Woods, R. J.; Dix, T. A. Development of a peptide-derived orally-active kappa-opioid receptor agonist targeting peripheral pain. *Open Med Chem J* **2013,** 7, 16-22.

80. Chavkin, C.; Goldstein, A. Specific receptor for the opioid peptide dynorphin: structure--activity relationships. *Proc Natl Acad Sci U S A* **1981,** 78, 6543-7.

81. Wan, Q.; Murray, T. F.; Aldrich, J. V. A novel acetylated analogue of dynorphin A-(1-11) amide as a kappa-opioid receptor antagonist. *J Med Chem* **1999,** 42, 3011-3.

82. Bennett, M. A.; Murray, T. F.; Aldrich, J. V. Identification of arodyn, a novel acetylated dynorphin A-(1-11) analogue, as a kappa opioid receptor antagonist. *J Med Chem* **2002,** 45, 5617-9.

83. Schlechtingen, G.; Zhang, L.; Maycock, A.; DeHaven, R. N.; Daubert, J. D.; Cassel, J.; Chung, N. N.; Schiller, P. W.; Goodman, M. [Pro^{3}]Dyn A(1-11)-NH_2: a dynorphin analogue with high selectivity for the kappa opioid receptor. *J Med Chem* **2000,** 43, 2698-702.

84. Schlechtingen, G.; DeHaven, R. N.; Daubert, J. D.; Cassel, J.; Goodman, M. Structure-activity relationships of dynorphin analogs substituted in positions 2 and 3. *Biopolymers* **2003,** 71, 71-6.

85. Vig, B. S.; Murray, T. F.; Aldrich, J. V. A novel N-terminal cyclic dynorphin A analogue *cyclo*^{N,5}[Trp^{3},Trp^{4},Glu^{5}] dynorphin A-(1-11)NH_2 that lacks the basic N-terminus. *J Med Chem* **2003,** 46, 1279-82.

86. Patkar, K. A.; Yan, X.; Murray, T. F.; Aldrich, J. V. [N^{alpha}-benzylTyr^{1},*cyclo*(D-Asp^{5},Dap^{8})]- dynorphin A-(1-11)NH_2 cyclized in the "address" domain is a novel kappa-opioid receptor antagonist. *J Med Chem* **2005,** 48, 4500-3.

87. Aldrich, J. V.; Patkar, K. A.; Chappa, A. K.; Fang, W.; Audus, K. L.; Lunte, S. M.; Carey, A. N.; McLaughli, J. P. Development of centrally acting peptide analogs: structure-transport studies and pharmacological evaluation of analogs of the opioid peptide dynorphin A. Wilce J, editor. *Proc 4th Intrn Pept Symp* **2008,** www.peptidoz.org, M 64.

88. Aldrich, J. V.; Patkar, K. A.; McLaughlin, J. P. Zyklophin, a systemically active selective kappa opioid receptor peptide antagonist with short duration of action. *Proc Natl Acad Sci U S A* **2009,** 106, 18396-18401.

89. Saito, T.; Hirai, H.; Kim, Y. J.; Kojima, Y.; Matsunaga, Y.; Nishida, H.; Sakakibara, T.; Suga, O.; Sujaku, T.; Kojima, N. CJ-15,208, a novel kappa opioid receptor antagonist from a fungus, Ctenomyces serratus ATCC15502. *J Antibiot (Tokyo)* **2002,** 55, 847-54.

90. Kulkarni, S. S.; Ross, N. C.; McLaughlin, J. P.; Aldrich, J. V. Synthesis of cyclic tetrapeptide CJ 15,208: a novel kappa opioid receptor antagonist. *Adv Exp Med Biol* **2009,** 611, 269-70.

91. Ross, N. C.; Kulkarni, S. S.; McLaughlin, J. P.; Aldrich, J. V. Synthesis of CJ-15,208, a novel kappa-opioid receptor antagonist. *Tetrahedron Lett* **2010,** 51, 5020-5023.

92. Ross, N. C.; Reilley, K. J.; Murray, T. F.; Aldrich, J. V.; McLaughlin, J. P. Novel opioid cyclic tetrapeptides: Trp isomers of CJ-15,208 exhibit distinct opioid receptor agonism and short-acting κ opioid receptor antagonism. *Br J Pharmacol* **2012,** 165, 1097-108.

93. Aldrich, J. V.; Senadheera, S. N.; Ross, N. C.; Ganno, M. L.; Eans, S. O.; McLaughlin, J. P. The macrocyclic peptide natural product CJ-15,208 is orally active and prevents reinstatement of extinguished cocaine-seeking behavior. *J Nat Prod* **2013,** 76, 433-8.

94. Aldrich, J. V.; Kulkarni, S. S.; Senadheera, S. N.; Ross, N. C.; Reilley, K. J.; Eans, S. O.; Ganno, M. L.; Murray, T. F.; McLaughlin, J. P. Unexpected opioid activity profiles of analogues of the novel peptide kappa opioid receptor ligand CJ-15,208. *ChemMedChem* **2011,** 6, 1739-45.

95. Aldrich, J. V.; Senadheera, S. N.; Ross, N. C.; Reilley, K. A.; Ganno, M. L.; Eans, S. E.; Murray, T. F.; McLaughlin, J. P. Alanine analogues of [D-Trp]CJ-15,208: novel opioid activity profiles and prevention of drug- and stress-induced reinstatement of cocaine-seeking behaviour. *Br J Pharmacol* **2014,** 171, 3212-22.

96. Dolle, R. E.; Michaut, M.; Martinez-Teipel, B.; Seida, P. R.; Ajello, C. W.; Muller, A. L.; DeHaven, R. N.; Carroll, P. J. Nascent structure-activity relationship study of a diastereomeric series of kappa opioid receptor antagonists derived from CJ-15,208. *Bioorg Med Chem Lett* **2009,** 19, 3647-50.

97. Khaliq, T.; Senadheera, S. N.; Lunte, S. M.; Aldrich, J. V. Structure-metabolism relationships of novel macrocyclic peptide opioid receptor ligands. *48th ACS National Meeting & Exposition*, American Chemical Society: San Francisco, CA, 2014; pp MEDI-430.

98. Liederer, B. M.; Phan, K. T.; Ouyang, H.; Borchardt, R. T. Significant differences in the disposition of cyclic prodrugs of opioid peptides in rats and guinea pigs following IV administration. *J Pharm Sci* **2005,** 94, 2676-2687.

99. Ouyang, H.; Tang, F.; Siahaan, T. J.; Borchardt, R. T. A modified coumarinic acid-based cyclic prodrug of an opioid peptide: its enzymatic and chemical stability and cell permeation characteristics. *Pharm Res* **2002,** 19, 794-801.

100. Ogu, C. C.; Maxa, J. L. Drug interactions due to cytochrome P450 *Proceedings (Baylor University. Medical Center)* **2000,** 13, 421-423.

101. Meyer, R. P.; Gehlhaus, M.; Knoth, R.; Volk, B. Expression and function of cytochrome p450 in brain drug metabolism. *Curr Drug Metab* **2007,** 8, 297-306.

102. Passeleu-Le Bourdonnec, C.; Carrupt, P. A.; Scherrmann, J. M.; Martel, S. Methodologies to assess drug permeation through the blood-brain barrier for pharmaceutical research. *Pharm Res* **2013,** 30, 2729-56.

103. Zlokovic, B. V. The blood-brain barrier in health and chronic neurodegenerative disorders. *Neuron* **2008,** 57, 178-201.

104. Cacabelos, R. Pharmacogenomics in Alzheimer's disease. *Methods Mol Biol* **2008,** 448, 213-357.

105. Miksys, S.; Tyndale, R. F. Cytochrome P450-mediated drug metabolism in the brain. *J Psychiatry Neurosci* **2013,** 38, 152-63.

106. Rubin, L. L.; Staddon, J. M. The cell biology of the blood-brain barrier. *Annu Rev Neurosci* **1999,** 22, 11-28.

107. Matter, K.; Balda, M. S. Signalling to and from tight junctions. *Nat Rev Mol Cell Biol* **2003,** 4, 225-36.

108. Alavijeh, M. S.; Chishty, M.; Qaiser, M. Z.; Palmer, A. M. Drug metabolism and pharmacokinetics, the blood-brain barrier, and central nervous system drug discovery. *NeuroRx* **2005,** 2, 554-571.

109. Banks, W. A.; Gertler, A.; Solomon, G.; Niv-Spector, L.; Shpilman, M.; Yi, X.; Batrakova, E.; Vinogradov, S.; Kabanov, A. V. Principles of strategic drug delivery to the brain (SDDB): development of anorectic and orexigenic analogs of leptin. *Physiol Behav* **2011,** 105, 145-9.

110. Pajouhesh, H.; Lenz, G. R. Medicinal chemical properties of successful central nervous system drugs. *NeuroRx* **2005,** 2, 541-53.

111. Kastin, A. J.; Akerstrom, V.; Pan, W. Interactions of glucagon-like peptide-1 (GLP-1) with the blood-brain barrier. *J Mol Neurosci* **2002,** 18, 7-14.

112. Jones, A. R.; Shusta, E. V. Blood-brain barrier transport of therapeutics via receptor-mediation. *Pharm Res* **2007,** 24, 1759-1771.

113. Potschka, H. Role of CNS efflux drug transporters in antiepileptic drug delivery: overcoming CNS efflux drug transport. *Adv Drug Deliv Rev* **2012,** 64, 943-52.

114. Sjostedt, N.; Kortejarvi, H.; Kidron, H.; Vellonen, K. S.; Urtti, A.; Yliperttula, M. Challenges of using in vitro data for modeling P-glycoprotein efflux in the blood-brain barrier. *Pharm Res* **2014,** 31, 1-19.

115. Ouyang, H.; Andersen, T. E.; Chen, W.; Nofsinger, R.; Steffansen, B.; Borchardt, R. T. A comparison of the effects of P-glycoprotein inhibitors on the blood-brain barrier permeation of cyclic prodrugs of an opioid peptide (DADLE). *J Pharm Sci* **2009,** 98, 2227-36.

116. Bellwon, P.; Culot, M.; Wilmes, A.; Schmidt, T.; Zurich, M. G.; Schultz, L.; Schmal, O.; Gramowski-Voss, A.; Weiss, D. G.; Jennings, P.; Bal-Price, A.; Testai, E.; Dekant, W. Cyclosporine A kinetics in brain cell cultures and its potential of crossing the blood-brain barrier. *Toxicol In Vitro* **2015**.

117. Jonker, J. W.; Wagenaar, E.; van Deemter, L.; Gottschlich, R.; Bender, H. M.; Dasenbrock, J.; Schinkel, A. H. Role of blood-brain barrier P-glycoprotein in limiting brain accumulation and sedative side-effects of asimadoline, a peripherally acting analgaesic drug. *Br J Pharmacol* **1999,** 127, 43-50.

118. Taillardat-Bertschinger, A.; Martinet, C. M.; Carrupt, P.-A.; Reist, M.; Caron, G.; Fruttero, R.; Testa, B. Molecular factors influencing retention on immobilized artificial membranes (IAM) compared to partitioning in liposomes and n-octanol. *Pharm Res* **2002,** 19, 729-737.

119. Di, L.; Kerns, E. H.; Bezar, I. F.; Petusky, S. L.; Huang, Y. Comparison of blood-brain barrier permeability assays: in situ brain perfusion, MDR1-MDCKII and PAMPA-BBB. *J Pharm Sci* **2009,** 98, 1980-91.

120. Audus, K. L.; Borchardt, R. T. Characterization of an in vitro blood-brain barrier model system for studying drug transport and metabolism. *Pharm Res* **1986,** 3, 81-7.

121. Sorensen, M.; Steenberg, B.; Knipp, G. T.; Wang, W.; Steffansen, B.; Frokjaer, S.; Borchardt, R. T. The effect of β-turn structure on the permeation of peptides across monolayers of bovine brain microvessel endothelial cells. *Pharm Res* **1997,** 14, 1341-1348.

122. Lippmann, E. S.; Azarin, S. M.; Kay, J. E.; Nessler, R. A.; Wilson, H. K.; Al-Ahmad, A.; Palecek, S. P.; Shusta, E. V. Derivation of blood-brain barrier endothelial cells from human pluripotent stem cells. *Nat Biotechnol* **2012,** 30, 783-91.

123. Egleton, R. D.; Mitchell, S. A.; Huber, J. D.; Janders, J.; Stropova, D.; Polt, R.; Yamamura, H. I.; Hruby, V. J.; Davis, T. P. Improved bioavailability to the brain of glycosylated Met-enkephalin analogs. *Brain Res* **2000,** 881, 37-46.

124. Weber, S. J.; Greene, D. L.; Sharma, S. D.; Yamamura, H. I.; Kramer, T. H.; Burks, T. F.; Hruby, V. J.; Hersh, L. B.; Davis, T. P. Distribution and analgesia of [^{3}H][D-Pen^{2},D-Pen^{5}]enkephalin and two halogenated analogs after intravenous administration. *J Pharmacol Exp Ther* **1991,** 259, 1109-17.

125. Horan, P. J.; Mattia, A.; Bilsky, E. J.; Weber, S.; Davis, T. P.; Yamamura, H. I.; Malatynska, E.; Appleyard, S. M.; Slaninova, J. Antinociceptive profile of biphalin, a dimeric enkephalin analog. *J Pharmacol Exp Ther* **1993,** 265, 1446-54.

126. Egleton, R. D.; Abbruscato, T. J.; Thomas, S. A.; Davis, T. P. Transport of opioid peptides into the central nervous system. *J Pharm Sci* **1998,** 87, 1433-1439.

127. Abbruscato, T. J.; Williams, S. A.; Misicka, A.; Lipkowski, A. W.; Hruby, V. J.; Davis, T. P. Blood-to-central nervous system entry and stability of biphalin, a unique double-enkephalin analog, and its halogenated derivatives. *J Pharmacol Exp Ther* **1996,** 276, 1049-57.

128. Witt, K. A.; Huber, J. D.; Egleton, R. D.; Davis, T. P. Insulin enhancement of opioid peptide transport across the blood-brain barrier and assessment of analgesic effect. *J Pharmacol Exp Ther* **2000,** 295, 972-978.

129. Bak, A.; Gudmundsson, O. S.; Friis, G. J.; Siahaan, T. J.; Borchardt, R. T. Acyloxyalkoxy-based cyclic prodrugs of opioid peptides: evaluation of the chemical and enzymatic stability as well as their transport properties across Caco-2 cell monolayers. *Pharm Res* **1999,** 16, 24-9.

130. Gudmundsson, O. S.; Nimkar, K.; Gangwar, S.; Siahaan, T.; Borchardt, R. T. Phenylpropionic acid-based cyclic prodrugs of opioid peptides that exhibit metabolic stability to peptidases and excellent cellular permeation. *Pharm Res* **1999,** 16, 16-23.

131. Gudmundsson, O. S.; Pauletti, G. M.; Wang, W.; Shan, D.; Zhang, H.; Wang, B.; Borchardt, R. T. Coumarinic acid-based cyclic prodrugs of opioid peptides that exhibit metabolic stability to peptidases and excellent cellular permeability. *Pharm Res* **1999,** 16, 7-15.

132. Joshi, A. Synthesis and biological evaluation of dynorphin analogs and, Caco-2 permeability of opioid macrocyclic tetrapeptides. Ph.D Dissertation, University of Kansas, Lawrence, KS, 2013.

Chapter II: Design and Synthesis of CJ-15,208 Analogs to Probe and Modify Pharmacokinetic Properties

2.1 Introduction

Our research focuses on the design and synthesis of orally active kappa (κ) opioid receptor (KOPr) ligands for the treatment of drug and alcohol addiction. For a general overview of the KOPr, its ligands, and their potential indications in pain, addiction, and depression, as well as background on our lead compound CJ-15,208, please refer to chapter 1.

The natural product macrocyclic tetrapeptide CJ-15,208 was reported to be a KOPr antagonist with modest affinity and selectivity for the KOPr.[1] We synthesized both the L- and D-Trp isomers of CJ-15,208 in our laboratory.[2, 3] The L-Trp isomer (the natural product) showed both agonist (antinociceptive) activity and short-acting KOPr antagonist activity *in vivo*,[4] while the D-Trp isomer showed predominantly KOPr antagonist activity *in vivo*.[5] Both isomers exhibited opioid activity in the central nervous system (CNS) after oral administration in mice.[5, 6] However, this required relatively high doses (30-60 mg/kg p.o.), and their antagonist activity was relatively short (<12 h). Our aim is to lower the dose necessary for these peptides to mediate central activity after oral administration while maintaining a desirable duration of action (preferably 12-24 h).

There are several pharmacokinetic properties that could be modulated to improve the bioavailability of these peptides. The first is stability to metabolism. While both peptides are stable to proteases in human plasma and whole blood, studies in mouse liver microsomes indicated that both peptides are susceptible to oxidation, presumably by cytochrome P450 (CYP-P450) enzymes, showing half-lives of about 60 min for the L-Trp isomer and 12 min for the D-Trp isomer.[7] Deuterated analogs can be useful in studying metabolites and patterns in metabolism. Further, *in vivo* resistance to oxidation can be improved by the incorporation of fluorine in appropriate

positions. Another property that can be modified is hydrophobicity, as CJ-15,208 and its D-Trp isomer both have very low aqueous solubility.[8] Structural modifications at hydrophobic residues such as Trp have been shown to improve the solubility of cyclic peptides.[9]

Therefore, this research focusing on improving the oral bioavailability of CJ-15,208 and its D-Trp analog has three components. The first was to synthesize deuterated analogs of the two leads as internal standards for use in studying the oxidative metabolism patterns. The second is to attenuate oxidative metabolism by incorporating fluorine into the aromatic residues of the two peptides. The third is to synthesize potential metabolites or analogs of metabolites by incorporating a hydroxyl group at the 5 position on Trp or a hydroxyl or methoxy functionality into one of the Phe residues. These analogs may be useful in elucidating the effects of oxidized metabolites on *in vivo* activity. They also have the potential benefit of increased aqueous solubility due to the incorporation of a polar functionality, which decreases the clogP from 5.0 (CJ-15,208) to 4.3 (hydroxylated analogs). The deuterated probes will be used for analysis in mouse liver microsomes, and the analogs incorporating fluorine, hydroxyl, and methoxy groups will be screened for activity *in vivo* and for affinity and selectivity *in vitro*.

2.2 Results and discussion

2.2.1 Fmoc protection

Fmoc (9-fluorenylmethoxycarbonyl) protection was required of specialty amino acids obtained in their free amino acid form, including L-phenyl-d_5-alanine, L-3-methoxyphenylalanine, L-*m*-tyrosine, 5-hydroxy-L-tryptophan, L-tryptophan-2′,4′,5′,6′,7′-d_5, D-tryptophan-2′,4′,5′,6′,7′-d_5, 5-fluoro-D-tryptophan, and 5-fluoro-D/L-tryptophan. All of these amino acids were protected using 9-fluorenylmethyl *N*-succinimidyl carbonate (Fmoc-OSu). Other specialty amino acids were obtained in the Fmoc-protected form.

The solubilities and stabilities of the tryptophan analogs differed from those of the phenylalanine analogs, which necessitated different reaction conditions. The procedure for protecting the tryptophan analogs was modified from Lawson *et al*.[10] The solvent used for the reaction was tetrahydrofuran (THF):saturated $NaHCO_3$ (1:1), and the reaction was quenched after 2 h to prevent degradation of the tryptophan side chain. Additionally, 5-hydroxy-L-tryptophan is susceptible to photodegradation, and therefore its protection was performed under argon gas and with the reaction vessel wrapped in aluminum foil. Yields of Fmoc protection of the Trp analog amino acids ranged from 24-90%.

The procedure for protecting the phenylalanine analogs was modified from Kang *et al*.[11] The solvent used for the reaction was dioxane: H_2O (1:1) with 3 equivalent $NaHCO_3$. Purification of the Phe analog amino acids was limited by the co-elution of unreacted Fmoc-OSu with the desired products. This difficulty was circumvented by using a small excess of the amino acid (1.1 equiv) and allowing the reactions to proceed for longer times, up to 15 h. Yields of Fmoc protection of the Phe analog amino acids ranged from 24-48%.

2.2.2 Peptide synthesis

The synthesis of 16 macrocyclic tetrapeptides was modified from previously reported procedures.[3, 12] The analogs of CJ-15,208 were synthesized on a relatively small scale, obtaining 1-110 mg (3-57% yield) of pure peptide (≥97% pure). Analogs with modifications at the Trp residue had linear precursor with the sequences R^{1*}-Phe-D-Pro-Phe were prepared, where R^1* was L-Trp(5-OH), L-Trp(d_5), D-Trp(d_5), Trp(5-F), or D-Trp(5-F), while for analogs with mono-substitutions at Phe^1 or Phe^3 the linear precursor sequences synthesized were Trp*-R^2-D-Pro-R^3, where R^2 or R^3 was Phe(d_5), Phe(3-F), Phe(4-F), *m*-Tyr, *m*-Tyr(Me), or Tyr(Me). An old batch of a high load chlorotrityl chloride resin (0.84 mmol/g) was observed to result in low yields of linear

peptides. It was used for the synthesis of some analogs (peptides **1a-4a**, **6a-8a**, Table 2.4) which had lower yields (5-60%) and in some cases lower purity (76.5% for peptide **8a**). The stabilities of the analogs to heat were unknown, so cyclizations were performed for 37.5-70.5 h at room temperature for these initial studies.

Scheme 2.1: Example synthesis of a macrocyclic tetrapeptide (peptide **4**)

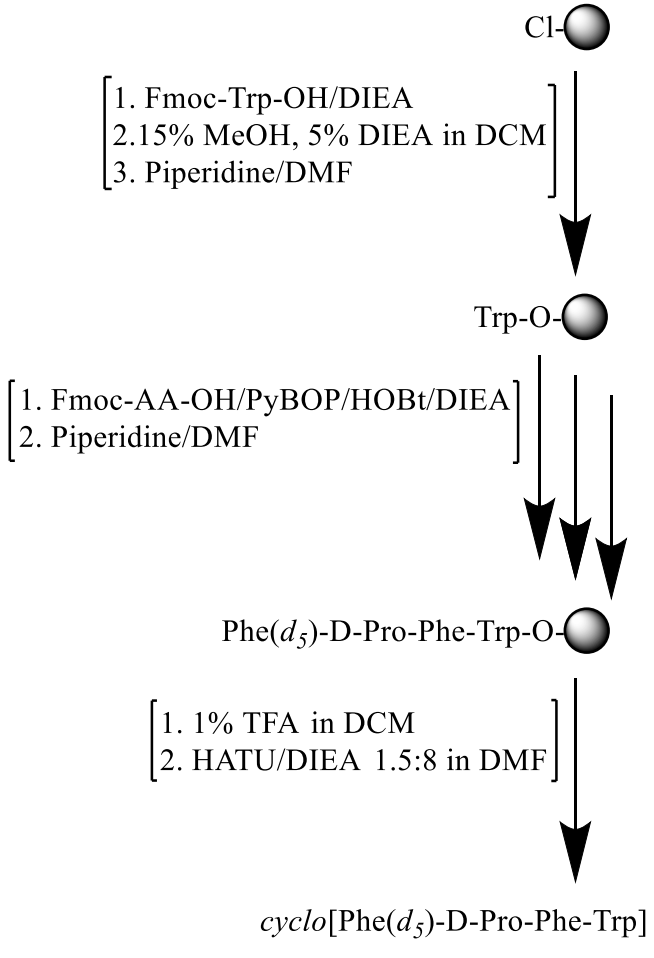

Table 2.1: Structures of cyclic CJ-15, 208 analogs and the corresponding linear precursor peptides

	Cyclic Peptides		Linear Precursor Sequence
1	*cyclo*[Trp(5-OH)-Phe-D-Pro-Phe]	**1a**	Trp(5-OH)-Phe-D-Pro-Phe-OH
2	*cyclo*[Trp(d_5)-Phe-D-Pro-Phe]	**2a**	Trp(d_5)-Phe-D-Pro-Phe-OH
3	*cyclo*[D-Trp(d_5)-Phe-D-Pro-Phe]	**3a**	D-Trp(d_5)-Phe-D-Pro-Phe-OH
4	*cyclo*[Phe(d_5)-D-Pro-Phe-Trp]	**4a**	Phe(d_5)-D-Pro-Phe-Trp-OH
5	*cyclo*[Phe-D-Pro-Phe(d_5)-Trp]	**5a**	Phe-D-Pro-Phe(d_5)-Trp-OH
6	*cyclo*[Trp(5-F)-Phe-D-Pro-Phe]	**6a**	Trp(5-F)-Phe-D-Pro-Phe-OH
7	*cyclo*[D-Trp(5-F)-Phe-D-Pro-Phe]	**7a**	D-Trp(5-F)-Phe-D-Pro-Phe-OH
8	*cyclo*[Phe(3-F)-D-Pro-Phe-Trp]	**8a**	Phe(3-F)-D-Pro-Phe-Trp-OH
9	*cyclo*[Phe-D-Pro-Phe(3-F)-Trp]	**9a**	Phe-D-Pro-Phe(3-F)-Trp-OH
10	*cyclo*[Phe(4-F)-D-Pro-Phe-Trp]	**10a**	Phe(4-F)-D-Pro-Phe-Trp-OH
11	*cyclo*[Phe-D-Pro-Phe(4-F)-Trp]	**11a**	Phe-D-Pro-Phe(4-F)-Trp-OH
12	*cyclo*[*m*-Tyr-D-Pro-Phe-Trp]	**12a**	*m*-Tyr-D-Pro-Phe-Trp-OH
13	*cyclo*[*m*-Tyr(Me)-D-Pro-Phe-Trp]	**13a**	*m*-Tyr(Me)-D-Pro-Phe-Trp-OH
14	*cyclo*[Phe-D-Pro-*m*-Tyr(Me)-Trp]	**14a**	Phe-D-Pro-*m*-Tyr(Me)-Trp-OH
15	*cyclo*[Tyr(Me)-D-Pro-Phe-Trp]	**15a**	Tyr(Me)-D-Pro-Phe-Trp-OH
16	*cyclo*[Phe-D-Pro-Tyr(Me)-Trp]	**16a**	Phe-D-Pro-Tyr(Me)-Trp-OH

Crude linear peptides were used for cyclization. The two diastereomeric linear precursor peptides **6a** and **7a** resulting from incorporating racemic 5-fluoro-D/L-tryptophan were not separated, and instead the resulting cyclic peptides were separated after cyclization. 5-Fluoro-D-tryptophan was used to synthesize a standard for peptide **7**, which allowed unambiguous identification of the two diastereomeric macrocyclic tetrapeptides **6** and **7** after purification.

It should be noted here that the peptides **1** and **12** were synthesized using amino acids with unprotected hydroxyl groups on their side chains. These residues were incorporated at the N-termini of the linear peptides, insuring the hydroxyls would not interfere with the coupling reactions. These hydroxyls were not observed to produce any by-products during the cyclization reaction that were not observed for the other analogs.

Peptide **1**, which contains 5-hydroxy-Trp, was found to be light sensitive and underwent oxidative degradation. It was protected from light with aluminum foil during synthesis of the

precursor linear peptide, cyclization, and lyphilization, and the cyclization reaction was also performed under argon gas. The crude linear peptide and cyclic peptide were stored under argon gas, as the unlyophilized (oil form) linear or cyclic peptides stored under nitrogen and protected from light showed evidence of degradation (red coloring) after 1 week. Lyophilization and storage at 0 ^{o}C was found to slow degradation. The oxidative degradation of peptide **1**, its linear precursor, and Fmoc-5-hydroxy-Trp itself resulted in the formation of at least one red-colored polar product. High-performance liquid chromatography (HPLC) analysis of peptide **1** that had undergone moderate oxidative degradation showed three less polar side products. The structures of these side products have not yet been elucidated.

2.2.3 Purification of macrocyclic tetrapeptides

The cyclic peptides were first purified by normal-phase flash chromatography as reported in previous studies. However, many of the peptides co-eluted with a yellow-colored HATU (2-(1H-7-azabenzotriazol-1-yl)-1,1,3,3-tetramethyluronium hexafluorophosphate) by-product, which was less polar than the L-Trp analogs but more polar than the D-Trp analogs on thin layer chromatogram (TLC). This by-product was also observed in previous syntheses of macrocyclic tetrapeptides. Silica gel chromatography was not successful in separating some of the cyclic peptides from the HATU by-product using either hexanes/ethyl acetate (EtOAc) or dichloromethane (DCM)/methanol as the solvent systems. This resulted in low yields of pure product for peptides **3** (4%) and **7** (3%), which also had the added difficulty of very small-scale syntheses (≤50 mg linear precursor) and which did not undergo further purification steps. Because most of the L-Trp macrocyclic tetrapeptides have limited solubility, selective precipitation was utilized for some peptides to prevent loss of the product by further chromatography. The HATU by-product was found to be more soluble in all of the solvents utilized than the cyclic peptides.

Some peptides, especially peptide **12**, were partially soluble in the solvents utilized, resulting in lower yields (4% for peptide **12**). Impure peptide that did not precipitate was concentrated or lyophilized for further purification. D-Trp analogs generally have greater solubility, so this procedure was not used for peptides **3** or **7**.

2.3 Conclusions and future studies

In conclusion, we designed and synthesized a series of macrocyclic CJ-15,208 analogs. Peptides incorporating deuterated Phe or Trp residues will be utilized to study oxidative metabolism in mouse liver microsomes. Other analogs are undergoing testing for *in vivo* activity, and the results of these studies will indicate how well modifications at each of the Phe residues are tolerated. *In vitro* testing will be performed to determine the affinities and selectivities of these peptides for the KOPr.

2.4 Experimental section

2.4.1 Materials

Reagents for peptide synthesis were obtained from the following sources: Fmoc-protected amino acids, 2-chlorotrityl chloride resin, and coupling reagents HATU (2-(1H-7-azabenzotriazol-1-yl)-1,1,3,3-tetramethyluronium hexafluorophosphate) and PyBOP (benzotriazol-1-yloxytripyrrolidinophosphonium hexafluorophosphate) were obtained from Novabiochem (EMD), San Diego, CA; 1-hydroxybenzotriazole and *N*,*N*-diisopropylethylamine (DIEA) were from Fluka, Milwaukee, WI; TFA was purchased from Pierce, Rockford, IL; and HPLC-grade solvents were from Fisher Scientific, Pittsburgh, PA. Deuterated amino acids were obtained from C/D/N Isotopes Inc. (Pointe-Claire, Quebec, Canada). Other specialty amino acids were obtained

from Chem-Impex International Inc. (Wood Dale, IL). Standard Fmoc-protected L- and D- amino acids were obtained from Novabiochem ((EMD), San Diego, CA).

2.4.2 Fmoc protection of phenylalanine analogs

The experimental procedure was modified from Kang *et al*.[11] L-Phenyl-d_5-alanine, L-meta-methoxyphenylalanine, or L-meta-tyrosine (1.1 equiv) was dissolved in dioxane:H_2O (1:1) with Fmoc-OSu (1 equiv) and $NaHCO_3$ (3 equiv). The reaction was stirred at room temperature for 3-15 h (3 h for Fmoc-Phe(d_5)), monitored with TLC, and was then quenched with 20 mL each ice and chloroform, and the pH adjusted to 3 using concentrated HCl. The product was extracted using chloroform (3 X 50 mL) and concentrated under low pressure. The crude product was then dissolved in EtOAc (150 mL), and the solution washed with saturated $NaHCO_3$ solution (6 X 100 mL). The aqueous layer was adjusted to pH 4 using concentrated HCl; a white precipitate formed which was then filtered, dissolved in EtOAc (250 mL), and the solution washed with dilute HCl (pH 3, 3 X 50 mL). The product was dried over $MgSO_4$, filtered, and concentrated under low pressure. The protected amino acid was then purified over preloaded 24 g silica gel columns at 35 mL/min with a solvent system of 0-15% MeOH in DCM or 20-80% EtOAc in hexanes (Fmoc-Phe(d_5)) over 15 min or 25 min (Fmoc-Phe(d_5)) using a Teledyne Combi Flash Rf monitored at 254 and 280 nm. Details of the reaction and purification conditions, yields, and spectral data can be found in Table 2.2.

Table 2.2: Reaction and purification conditions of Fmoc-protected phenylalanine analogs and spectral data

Fmoc-AA	H-AA (mg)	Solvent[a] volume/ Reaction time (mL/h)	Chroma-tography solvent system	Pure product (mg)	% yield	HPLC (t_R(min)/ % purity)[b]	$[M+Na]^+$ ESI-MS (*m/z*) Observed (Calculated)
Fmoc-L-Phe(d_5)	300	24/3	20-80% EtOAc in hexanes	249	48	12.52/97.4	454.18 (454.18)
Fmoc-L-*m*-Tyr	500	40/15	0-15% MeOH in DCM	238	24	-[c]	426.13 (426.13)
Fmoc-L-*m*-Tyr(Me)	500	40/15	0-15% MeOH in DCM	297	31	12.40/91.3	415.17 (415.17)

[a]Dioxane:H_2O (1:1). [b]HPLC analysis using a solvent system of 30-70% Solvent B over 40 min (Solvent A= H_2O; Solvent B= MeCN, both containing 0.1% TFA). [c]Purity is being determined.

2.4.3 Fmoc protection of tryptophan analogs

The experimental procedure was modified from Lawson, *et al.*[10] One equivalent of unprotected tryptophan analogs, including 5-hydroxy-L-tryptophan, L-tryptophan-2′,4′,5′,6′,7′-d_5, D-tryptophan-2′,4′,5′,6′,7′-d_5, 5-fluoro-D-tryptophan, or 5-fluoro-D/L-tryptophan, and Fmoc-OSu (1.2 or 2 equiv) were suspended in THF:saturated $NaHCO_3$ (1:1). The solvents were degassed for 5-hydroxy-L-tryptophan, and the reaction with this amino acid was kept under argon gas and protected from light with aluminum foil. The reaction was stirred at room temperature for 2 h. The THF was removed under low pressure, and the pH of the resulting aqueous suspension adjusted to $\leq$ 3 using concentrated HCl. The aqueous solution was extracted with EtOAc (2 X, 150 mL). The organic layer was dried over $MgSO_4$ and concentrated at low pressure.

The amino acids were then purified over silica gel using a Teledyne Combi Flash Rf system with monitoring at 254 and 280 nm. Fmoc-L-Trp(d_5) and Fmoc-L-Trp(d_5) were purified over preloaded 24 g silica gel columns at 35 mL/min using 20-100% EtOAc in hexanes over 25 min. Fmoc-D-Trp(5-F) and Fmoc-DL-Trp(5-F) were purified over a preloaded 24 or 4 g (Fmoc-D-Trp(5-F)) silica gel column at 35 mL/min of 18 mL/min using (Fmoc-D-Trp(5-F)) 20-100% EtOAc in hexanes over 25 min. Fmoc-L-Trp(5-OH) was purified over preloaded 24 g silica gel

columns at 35 mL/min using 25-100% EtOAc in hexanes over 25 min. The amino acid was then re-dissolved in H_2O:MeCN (approximately 3:1, 4-8 mL), and the solutions transferred to scintillation vials, frozen and lyophilized. (Solutions of Fmoc-5-hydroxy-L-tryptophan was covered with aluminum foil during lyphilization.) Specific reaction and purification conditions, analytical, and spectral data can be found in Table 2.3.

Table 2.3: Reaction and purification conditions of Fmoc-protected tryptophan analogs and spectral data

Fmoc-AA	H-AA (mg)	Solvent[b] volume (mL)	Chromatography solvent system	Pure product (mg)	% yield	UPLC (t_R (min)/% Purity)[c]	$[M+Na]^+$ ESI-MS (m/z) Observed (Calculated)
Fmoc-L-Trp(d_5)	50	2	20-100% EtOAc in hexanes	73.5	71	6.47/92.5[d]	454.18(454.18)
Fmoc-D-Trp(d_5)	50	2	20-100% EtOAc in hexanes	93.2	90	6.47/>99[d]	454.18(454.18)
Fmoc-D-Trp (5-F)	50	2	20-100% EtOAc in hexanes	23.7	24	6.61/96.3[e]	467.14(467.14)
Fmoc-DL-Trp (5-F)	400	16	20-100% EtOAc in hexanes	330.9	41	6.63/98.3[e]	467.14(467.14)
Fmoc-L-Trp (5-OH)[a]	500	24	25-100% EtOAc in hexanes	564.8	56	4.03/96.9[d,e]	465.14(465.18)

[a]The reaction was performed protected from the light under argon gas. [b]THF:saturated $NAHCO_3$ (1:1), [c]UPLC analysis using a solvent system of 40-80% Solvent B over 14 min (Solvent A= H_2O; Solvent B= MeCN, both containing 0.1% TFA). [d]UPLC monitored at 280 nm. [e]UPLC monitored at 214 nm.

2.4.4 Linear peptide synthesis: general procedure

Linear peptide synthesis was performed as previously reported.[3, 12] All peptides were assembled on a high load 2-chlorotrityl chloride resin (0.84 or 1.1 mmol/g, 85-1000 mg) by SPPS using Fmoc-protected amino acids according to standard procedures. The resin was first swollen with 10 mL of DCM (2 X 10 min). Peptides were synthesized on a manual multiple peptide synthesizer ("CHOIR") constructed in house[13] using 15 mL polypropylene syringes fitted with a polytetrafluoroethylene (PTFE) frits. Attachment of the first amino acid to the resin was performed

using a twofold excess of amino acid and fivefold excess of DIEA in DCM:*N*,*N*-dimethylformamide (DMF) (4:1, 5 mL), which was allowed to agitate for 5-6 h. Any remaining active sites on the 2-chlorotrityl/chloride resin were deactivated by washing the resin with 15% MeOH and 5% DIEA in DCM (10 mL, 2 X 10 min). Following removal of the Fmoc protecting group using 20% piperidine in DMF for 20 min, the resin was washed in DMF, DCM:DMF (1:1), and DCM (10 mL, 5 X 30 sec each).

The Fmoc-protected amino acids were then coupled using 2-fold excess and the coupling reagents PyBOB, 1-hydroxybenzotriazole (HOBt), and DIEA (2:2:5 relative to the resin substitution) in 10 mL DCM:DMF (1:1) for 2-4 h. None of the side chains were protected. Completion of the coupling reactions was indicated by the qualitative ninhydrin and/or chloranil test.[14, 15] For peptide **1a**, photodegradation was minimized by covering the vessel with aluminum foil during all reactions and during storage.

2.4.5 Linear peptide cleavage

All linear peptides were cleaved from the resin using 1% TFA in DCM (100 mL) that was bubbled through the resin in 5 mL portions for 2 min each. The resin was then washed with DCM (2 X 4 mL). All of the cleavage solution was drained into a round-bottom flask, and the DCM was then evaporated to dryness. The crude linear peptide was then triturated with diethyl ether (3 X 10 mL), dried, re-dissolved in H_2O:MeCN (approximately 3:1, 4-8 mL) and the solutions transferred to scintillation vials, frozen and lyophilized. Yields of crude linear peptide ranged from 46-220 mg as white powders. The linear precursor of peptide **1** was protected from light using aluminum foil during cleavage, drying, and lyophilization. The linear peptides were analyzed by electrospray ionization mass spectrometry (ESI-MS) and ultra-performance liquid chromatography (UPLC, Table 2.4) as described below.

Table 2.4: Linear peptide yield and analytical data

Peptide	Resin (mg)	Peptide yield (mg)	% yield	HPLC (t_R (min)/% Purity)[c]	$[M+H]^+$ ESI-MS (*m/z*)	
					Calculated	Observed
1a[a]	500[b]	153.2	60	6.03/80.6[d]	612.28	612.28
2a	260[b]	56	44	6.30/>99[d,e]	601.32	601.32
3a	332[b]	46.2	28	7.03/>99[d,e]	601.32	601.32
4a	1000[b]	26.7	5	6.89/93.2[e]	601.32	601.32
5a	436	245.3	88	6.92/94.1[d]	601.32	601.32
6a 7a	500[b]	112.6	44	6.65/53.4, 7.01/46.6[d]	614.28	614.28
7a	85	52	96	7.24/98.4[e]	614.28	614.28
8a	400[b]	37	18	7.01/67.5[d,e]	614.28	614.28
9a	400	223.9	83	6.94/89.0[d]	614.28	614.24
10a	560	221.7	59	7.04/88.8[d]	614.28	614.28
11a	400	228.9	85	6.95/>99[d]	614.28	614.28
12a	358	136.7	57	6.28/96.5[e]	612.28	612.28
13a	215	101.6	69	7.04/94.0[d]	626.30	626.30
14a	215	124.4	84	6.94/97.0[d]	626.30	626.30
15a	544	216	58	6.87/95.6[e]	626.30	626.27
16a	400	219.9	80	6.83/>99[d,e]	626.30	626.26

Resin loading was 1.1 mmol/g. [a]Protected from the light. [b]0.84 mmol/g resin loading. [c]UPLC analysis using a solvent system of 20-80% Solvent B over 14 min (Solvent A= H_2O; Solvent B= MeCN, both containing 0.1% TFA). [d]UPLC monitored at 280 nm. [e]UPLC monitored at 214 nm.

2.4.6 Cyclization of linear tetrapeptides

Cyclization procedures were modified from previously reported methods.[3, 12] Half of the crude linear peptide (1 equiv for this purpose) in DMF (10-20 mL) was added dropwise at a rate of 1.2 mL/h (using a KD Scientific single infusion syringe pump) to a dilute solution of HATU (1.5 equiv) and DIEA (8 equiv) in DMF. Additional HATU (1.5 equiv) and DIEA (8 equiv) was then added to the reaction in one portion, and the second half of the linear peptide (1 equiv) in DMF (10-20 mL) was added dropwise at a rate of 1.2 mL/h, as described above. The linear precursors **7a**, **9a-12a** were delivered in one portion (20 mL DMF) at 0.5 mL/h. The final concentrations after additions of the linear peptide, HATU, and DIEA in DMF were 1, 1.5, and 8

mM, respectively. The total reaction times were 37.5-70.5 h. Peptide **1** was cyclized under argon gas and protected from light with aluminum foil.

The solvent was evaporated under reduced pressure at 37 °C, the resulting residue was dissolved in EtOAc (100 mL), and the organic phase washed sequentially with 1 N citric acid, saturated $NaHCO_3$ solution, and brine (3 X each). The organic phase was dried over anhydrous $MgSO_4$, and the filtrate evaporated under reduced pressure to give the crude macrocyclic tetrapeptide, which was purified by silica gel chromatography with gradients of EtOAc in hexanes or MeOH in DCM using a Teledyne Combi Flash Rf system and monitoring at 254 and 280 nm. Peptides **1**, **5-6**, and **9-16** underwent an additional purification step by selective precipitation with EtOAc (peptide **1**), 25% MeCN in H_2O (peptides **5-6**, **9-11**, and **13-16**), or 100% MeCN (peptide **12**). The peptide was then dried and re-dissolved in H_2O:MeCN (approximately 2:1, 4-8 mL) and the solutions transferred to scintillation vials, frozen and lyophilized. Yields of pure cyclic peptide (≥97% pure) ranged from 1-110 mg (4-57% yield) as white powders. Specific reaction conditions, purification methods, and yields are listed in Table 2.5.

Table 2.5: Cyclization and purification conditions for the cyclic peptides and yields of the pure peptides

Peptide	Linear peptide (mg)[a]	Linear peptide delivery (mM/mL)	Reaction time (h)	Chromatography solvent system	Solvent precipitation	Yield (pure) (mg)	% Yield (pure)
1	120[b]	4.9/20[c]	67.5	0-5% MeOH in DCM	EtOAc	21.1	18
2	50	4.3/10[c]	37.5	40-100% EtoAc in hexanes	-	16.6	34
3	40	3.3/10[c]	37.5	30-100% EtoAc in hexanes	-	20	52
4	24	2.0/10[c]	47	35-100% EtoAc in hexanes	-	0.93	4
5	240	10/20[c]	48	0-5% MeOH in DCM	20% MeCN in H_2O	121.8	52
6, 7	100	4.1/20[c]	70.5	20-100% EtoAc in hexanes	20%MeCN in H_2O (**6**)	6.2 (**6**) 9.7 (**7**)	13 (**6**) 20 (**7**)
7	50	4.1/20[d]	68.5	0-5% MeOH in DCM	-	1.3	3
8	35	1.4/20[c]	47	35-100% EtoAc in hexanes	-	4.1	12
9	200	16/20[d]	45	0-5% MeOH in DCM	20% MeCN in H_2O	50	26
10	200	16/20[d]	48	35-100% EtoAc in hexanes	20% MeCN in H_2O	34.5	18
11	200	16//20[d]	64	0-5% MeOH in DCM	20% MeCN in H_2O	54.8	28
12	130	11/20[d]	68.5	0-10% MeOH in DCM	MeCN	5.4	4
13	100	4.0/20[c]	48	0-5% MeOH in DCM	20% MeCN in H_2O	30.9	32
14	100	4.0/20[c]	48	0-5% MeOH in DCM	20% MeCN in H_2O	33	34
15	200	8.0/20[c]	48	0-5% MeOH in DCM	20% MeCN in H_2O	46.5	24
16	200	8.0/20[c]	48	0-5% MeOH in DCM	20% MeCN in H_2O	110	57

[a]The final concentrations of linear peptide, HATU, and DIEA in DMF were 1, 1.5, and 8.0 mM, respectively; the reactions were performed at room temperature. [b]The reaction was performed under argon gas and protected from light. [c]The linear peptide was delivered in two portions at 1.2 mL/h. [d]The linear peptide was delivered in one portion at 0.5 mL/h.

2.4.7 HPLC, UPLC, and MS analysis

Mass spectra of the protected amino acids, the macrocyclic tetrapeptides, and their linear precursors were obtained on a Waters LCT Premier ESI time of flight mass spectrometer.

The purity of Fmoc-protected tryptophan analogs and the linear peptides was verified on a Waters Acquity H-class UPLC chromatograph equipped with Quaternary Solvent Manager, Sample Manager FTN and TUV Detector. An Acquity UPLC BEH C18 column (1.7 μ, 130 Å, 2.1 x 50 mm) equipped with an Acquity UPLC BEH C18 VanGuard pre-column (1.7 μ, 130 Å, 2.1 x 5 mm) was used with a flow rate of 0.2 mL/min. A gradient of 40-80% MeCN in H_2O over 14 min was used for the protected tryptophan analogs (Table 2.3) and 20-80% MeCN in H_2O over 14 min was used for the linear peptides (Table 2.4). Solutions of peptides or amino acids were injected at a volume of 0.5-10 μL and detected at 214 and 280 nm. Chromatographic data were acquired and analyzed using Waters Empower 3 software. Spectral data can be found in Table 2.3 for the Fmoc-protected amino acids and in Table 2.4 for the linear peptide precursors.

The Fmoc-protected Phe analogs and the macrocyclic tetrapeptides were analyzed using an Agilent 1200 series liquid chromatograph system equipped with a multiple wavelength UV-Vis detector. HPLC analyses were performed on a Vydac 218TP C18 column (5 μ, 4.6 x 50 mm) at a flow rate of 1 mL/min. The Fmoc-protected Phe analogs were analyzed using a solvent system of 30-70% Solvent B over 40 min (Solvent A= H_2O; Solvent B= MeCN, both containing 0.1% TFA). The macrocyclic peptides were analyzed using two different solvent systems: system 1: 15-55% MeCN containing 0.1% TFA over 40 min, system 2: 30-70% MeOH over 40 min, with detection at 230 and 280 nm for both systems. Spectral data for the cyclic peptides can be found in Table 2.6.

Table 2.6: Analytical data for the cyclic peptides

Peptide	HPLC (t_R (min)/% Purity)		$[M+Na]^+$ ESI-MS (*m*/*z*)	
	System 1[c]	System 2[d]	Calculated	Observed
1	12.46/>99	9.93/>99	616.25	616.26
2	18.78/>99	18.74/>99	605.29	605.29
3	26.09/>99	27.54/>99	605.29	605.29
4	18.82/97.9	19.56/>99	605.29	605.29
5	18.70/>99	19.11/>99	605.29	605.29
6	20.17/>99	20.25/>99	618.25	618.25
7[a]	27.69/97.5	29.7/94.2	618.25	618.25
7[b]	27.57/>99	30.23/97.6	618.25	618.25
8	20.16/97.6	20.88/>99	618.25	618.25
9	19.81/>99	20.63/>99	618.25	618.25
10	19.86/98.4	20.86/>99	618.25	618.25
11	19.88/>99	20.87/>99	618.25	618.25
12	15.30/>99	13.39/>99	616.25	616.26
13	19.46/>99	20.65/>99	630.27	630.27
14	19.25/99.0	20.29/98.9	630.27	630.27
15	18.90/>99	19.98/>99	630.27	630.27
16	18.77/>99	19.96/>99	630.27	630.27

[a]Cyclized from D/L-Trp(5-F) mixture of linear precursors. [a]Cyclized from pure D-Trp(5-F) linear precursor. [c]System 1: 15-55% Solvent B over 40 min (Solvent A= H_2O; Solvent B= MeCN, both containing 0.1% TFA), [d]System 2: 30-70% Solvent B over 40 min (Solvent A= H_2O; Solvent B= MeOH, both containing 0.1% TFA), flow rate 1.0 mL/min.

2.5 References

1. Saito, T.; Hirai, H.; Kim, Y. J.; Kojima, Y.; Matsunaga, Y.; Nishida, H.; Sakakibara, T.; Suga, O.; Sujaku, T.; Kojima, N. CJ-15,208, a novel kappa opioid receptor antagonist from a fungus, Ctenomyces serratus ATCC15502. *J Antibiot (Tokyo)* **2002,** 55, 847-54.

2. Kulkarni, S. S.; Ross, N. C.; McLaughlin, J. P.; Aldrich, J. V. Synthesis of cyclic tetrapeptide CJ 15,208: a novel kappa opioid receptor antagonist. *Adv Exp Med Biol* **2009,** 611, 269-70.

3. Ross, N. C.; Kulkarni, S. S.; McLaughlin, J. P.; Aldrich, J. V. Synthesis of CJ-15,208, a novel kappa-opioid receptor antagonist. *Tetrahedron Lett* **2010,** 51, 5020-5023.

4. Ross, N. C.; Reilley, K. J.; Murray, T. F.; Aldrich, J. V.; McLaughlin, J. P. Novel opioid cyclic tetrapeptides: Trp isomers of CJ-15,208 exhibit distinct opioid receptor agonism and short-acting κ opioid receptor antagonism. *Br J Pharmacol* **2012,** 165, 1097-108.

5. Eans, S. O.; Ganno, M. L.; Reilley, K. J.; Patkar, K. A.; Senadheera, S. N.; Aldrich, J. V.; McLaughlin, J. P. The macrocyclic tetrapeptide [D-Trp]CJ-15,208 produces short-acting kappa opioid receptor antagonism in the CNS after oral administration. *Br J Pharmacol* **2013,** 169, 426-36.

6. Aldrich, J. V.; Senadheera, S. N.; Ross, N. C.; Ganno, M. L.; Eans, S. O.; McLaughlin, J. P. The macrocyclic peptide natural product CJ-15,208 is orally active and prevents reinstatement of extinguished cocaine-seeking behavior. *J Nat Prod* **2013,** 76, 433-8.

7. Khaliq, T.; Senadheera, S. N.; Lunte, S. M.; Aldrich, J. V. Structure-metabolism relationships of novel macrocyclic peptide opioid receptor ligands. *48th ACS National Meeting & Exposition*, American Chemical Society: San Francisco, CA, 2014; pp MEDI-430.

8. Joshi, A. Synthesis and biological evaluation of dynorphin analogs and, Caco-2 permeability of opioid macrocyclic tetrapeptides. Ph.D Dissertation, University of Kansas, Lawrence, KS, 2013.

9. Kucharczyk, N.; Thurieau, C.; Paladino, J.; Morris, A. D.; Bonnet, J.; Canet, E.; Krause, J. E.; Regoli, D.; Couture, R.; Fauchere, J. L. Tetrapeptide tachykinin antagonists: synthesis and modulation of the physicochemical and pharmacological properties of a new series of partially cyclic analogs. *J Med Chem* **1993,** 36, 1654-61.

10. Lawson, K. V.; Rose, T. E.; Harran, P. G. Template-induced macrocycle diversity through large ring-forming alkylations of tryptophan. *Tetrahedron* **2013,** 69, 7683-7691.

11. Kang, S.-U.; Worthy, K. M.; Bindu, L. K.; Zhang, M.; Yang, D.; Fisher, R. J.; Burke, T. R., Jr. Design and synthesis of 4-(α-Hydroxymalonyl)phenylalanine as a new phosphotyrosyl

mimetic and its use in gowth factor receptor bound 2 Src-Homology 2 (Grb2 SH2) domain-binding peptides. *J Med Chem* **2005,** 48, 5369-5372.

12. Aldrich, J. V.; Kulkarni, S. S.; Senadheera, S. N.; Ross, N. C.; Reilley, K. J.; Eans, S. O.; Ganno, M. L.; Murray, T. F.; McLaughlin, J. P. Unexpected opioid activity profiles of analogues of the novel peptide kappa opioid receptor ligand CJ-15,208. *ChemMedChem* **2011,** 6, 1739-45.

13. Vig, B. S.; Aldrich, J. V. An inexpensive, manually operated, solid-phase, parallel synthesizer. *Aldrichimica Acta* **2004,** 37, 2.

14. Kaiser, E.; Colescott, R. L.; Bossinger, C. D.; Cook, P. I. Color test for detection of free terminal amino groups in the solid-phase synthesis of peptides. *Anal Biochem* **1970,** 34, 595-8.

15. Vojkovsky, T. Detection of secondary amines on solid phase. *Pept Res* **1995,** 8, 236-7.

Chapter III: CJ-15,208 and [D-Trp]CJ-15,208: Their Permeability Across Biological Barriers and Interaction with P-glycoprotein

3.1 Introduction

We are interested in orally bioavailable and centrally acting peptidic ligands for kappa opioid receptors (KOPr) as potential treatments for drug abuse and pain. For background on our two lead compounds, CJ-15,208 and [D-Trp]CJ-15,208, their activities and metabolic stabilities please see section 1.3. While these compounds have shown central activity after oral delivery in mice, this activity requires high doses.[1, 2] We would like to identify the factors limiting central exposure of these peptides in order to design analogs with greater membrane permeability and CNS levels.

Previous studies in our laboratory using Caco-2 cell monolayers indicated that both CJ-15,208 and [D-Trp]CJ-15,208 are permeable across biological barriers, with P_{app} (apparent permeability coefficient) values of 3.2 x 10^{-6} cm/sec (A to B) and 18.9 x 10^{-6} cm/sec (B to A) for the L-Trp isomer and 25.5 x 10^{-6} cm/sec (A to B) and 22.7 x 10^{-6} cm/sec (B to A) for the D-Trp isomer.[3] CJ-15,208 appeared to be effluxed, with a P_{app} ratio ((B to A)/(A to B)) of 5.9, but these studies did not identify efflux proteins interacting with CJ-15,208. It was hypothesized that P-glycoprotein (P-gp) may be involved in the observed efflux, as this protein interacts with many hydrophobic substrates and is present at the intestinal barrier and blood-brain barrier (BBB).[4] For an overview of the BBB, prominent BBB efflux proteins, and *in vitro* models of the BBB see section 1.4.

As a model of the intestinal barrier, Caco-2 cells have the advantage of being derived from a human intestinal cancer and of expressing a variety of efflux proteins.[5] However, Caco-2 cells require 21 days of development, and slow growth increases the risk of contamination and of the

monolayer becoming damaged. Madin-Darby canine kidney (MDCK) cells have been used as a faster alternative to Caco-2 cells for modeling the intestinal barrier.[6] While MDCK cells are derived from canine kidney cells and do not express efflux proteins at the same basal levels that are observed in Caco-2 cells,[7] they develop in 6 days and can be transfected to express human efflux proteins such as P-gp (gene MDR1). Additionally, while MDCK cells are models of the intestinal barrier, when they are transfected with efflux proteins present at the BBB, they can be used to predict permeability across the BBB.[8, 9] These cell lines have been successfully used to study cyclic opioid peptides.[10]

In this study, we used wild type MDCK cells (MDCK-WT) and MDCK cells transfected with the multidrug resistant gene 1 (MDR1) expressing human P-gp to determine the interactions of CJ-15,208 and [D-Trp]CJ-15,208 with P-gp. The two experiments performed with these cells were the rhodamine 123 (Rh 123) efflux assay, which uses the fluorescent P-gp efflux substrate Rh 123 to determine whether the peptides can inhibit P-gp efflux, and transwell transport across MDCK cell monolayers to determine whether the peptides are effluxed by P-gp.

3.2 Results and Discussion

3.2.1 Rhodamine 123 efflux studies

The MDCK-MDR1 cells were seeded on 24 wells plates, and monolayers were cultured for 6 days. On the 6th day the monolayer integrity was assessed visually, and then the monolayers preincubated with the vehicles, peptides, or the P-gp inhibitor verapamil for 30 min at 37 ^{o}C. Rh 123 was then added, and the monolayers incubated for another 60 min. The monolayers were then washed and lysed, and the fluorescence of Rh 123 in the cell lysate measured. The protein concentration of the lysate was measured using the bicinchoninic acid (BCA) assay, and the

fluorescence normalized for protein concentration to calculate the relative fluorescence units (RFU).

Vehicles to solubilize the analogs in Hank's balanced salt solution (HBSS) were chosen in previous Caco-2 studies.[3] CJ-15,208 and [D-Trp]CJ-15,208 were solubilized in 0.25% dimethylsulfoxide (DMSO) + *N*,*N*-dimethylacetamide (DMA) in HBSS (vehicle 1) or 0.25% DMSO + 2.25% *N*-methylpyrrolidone (NMP) in HBSS (vehicle 2), respectively. While these vehicles were successfully used in the Caco-2 assays, vehicle 2 appeared to affect the uptake of Rh 123 in unpredictable ways in initial studies (protein concentration was not measured during these initial studies). This vehicle consistently increased fluorescence without peptide, but when [D-Trp]CJ-15,208 was added, the fluorescence was decreased back to control levels (Figure 3.1). [D-Trp]CJ-15,208 was observed to form visible peptide aggregates in vehicle 1, and these aggregates appeared to potently inhibit P-gp efflux (Figure 3.1). The vehicle selected to solubilize [D-Trp]CJ-15,208 was 1% DMSO in HBSS, which did not appear to significantly affect Rh 123 uptake (Figure 3.1) and did not result in visible peptide aggregates. However, subsequent studies showed variability in the fluorescence in controls containing 1% DMSO in HBSS (data not shown). These experiments need to be repeated.

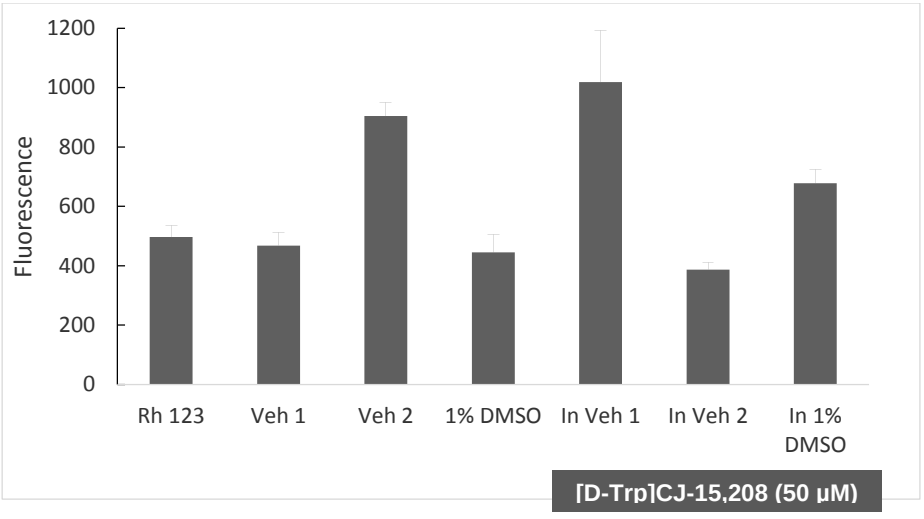

Figure 3.1: Initial data on the effect of [D-Trp]CJ-15,208 vehicles on the efflux of Rh 123 in MDCK-MDR1 cell monolayers (n = 2).

3.2.1.1 CJ-15,208 inhibition of Rh 123 efflux

CJ-15,208 was soluble in vehicle 1, and therefore this vehicle was used in studies of the effect of this peptide on Rh 123 efflux. A statistically significant increase in Rh 123 uptake was observed at 40 µM CJ-15,208 (Figure 3.2), suggesting that CJ-15,208 is an inhibitor of P-gp. The lower P-gp inhibition at 50 µM may be due to poor aqueous solubility of the compound.

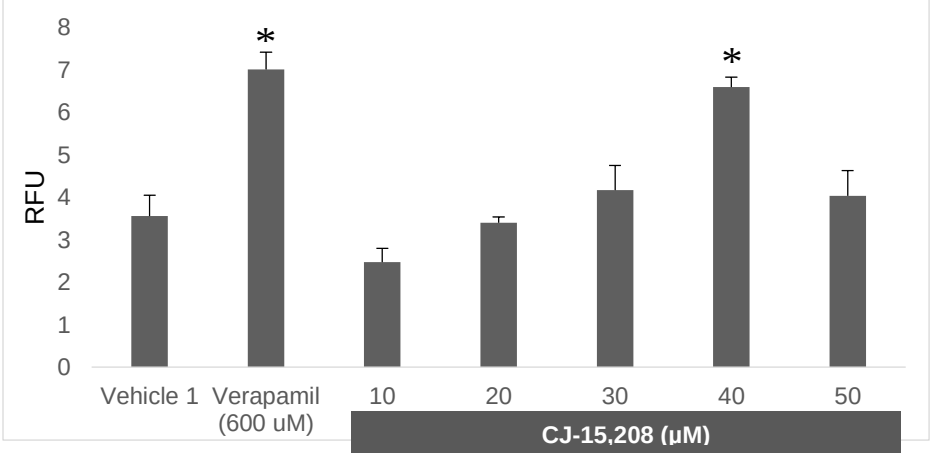

Figure 3.2: Initial data on the effect of CJ-15,208 on the efflux of Rh 123 in MDCK-MDR1 cell monolayers (n = 1). All compounds are in Vehicle 1. *Statistically different ($p < 0.05$) from vehicle 1, 1-way ANOVA.

3.2.2 Permeability studies

The transport of CJ-15,208 and [D-Trp]CJ-15,208 across MDCK cell monolayers was determined using quantification by UPLC-MS/MS. The MDCK-WT and MDCK-MDR1 cells were seeded on polycarbonate filters, and monolayers were cultured for 6 days. On the 6th day the monolayer integrity was assessed by measuring the transepithelial electrical resistance (TEER) and lucifer yellow (LY) transport (both P_{app} values and percent permeability over 1 h). TEER values of >200 Ω/cm^2 and a P_{app} values for LY of $\leq 0.5 \times 10^{-5}$ cm/sec were observed for MDCK-WT, which generally met the criteria used to indicate formation of tight junctions[11] and were consistent with previously reported values.[12] In these studies the MDCK-MDR1 cell mono-layers did not meet these criteria;[11] lower TEER values for MDCK-MDR1 cell monolayers have also been reported by others.[13] Therefore the criteria for MDCK-MDR1 cell monolayers in these studies were TEER values of >140 Ω/cm^2 and a P_{app} values for LY of $\leq 1.5 \times 10^{-5}$ cm/sec without GF-120918 (elacridar, 5 μM) and $\leq 2.5 \times 10^{-5}$ cm/sec with GF-120918.

CJ-15,208 and [D-Trp]CJ-15,208 were solubilized in the same vehicles used in the Rh 123 efflux studies, namely in vehicle 1 and 1% DMSO in HBSS, respectively, at a concentration of 50 μM. The transport experiments were conducted six days after seeding. For experiments utilizing the P-gp inhibitor GF-120918 (5 μM), the MDCK-MDR1 cell monolayers were incubated with the P-gp inhibitor for 20 min before the peptide was added.[14, 15] The transwells containing MDCK-WT or MDCK-MDR1 monolayers were incubated with the peptides in their respective vehicles for 2 h with samples collected for transport in both the apical to basolateral (A-B) and basolateral to apical (B-A) directions, followed by examining transport of LY in the A-B direction.

Concentrations of CJ-15,208 and [D-Trp]CJ-15,208 were quantified using liquid chromatography electrospray ionization tandem mass spectroscopy (LC-ESI-MS/MS) in positive

ion mode coupled to reversed phase ultra-high performance liquid chromatography (RP-UPLC). Following fragmentation, multiple reaction monitoring (MRM) was used to quantify the peptides.

Table 3.1: Results obtained from MDCK-WT and MDCK-MDR1 monolayer permeability experiments for CJ-15,208 and [D-Trp] CJ-15,208.

Cell/ condition (TEER value ranges)	**Peptide**	**Peptide transport** P_{app} cm/sec (x 10^{-5}) ± SEM		**Post-peptide LY transport** P_{app} cm/sec (x 10^{-5}) ± SEM (% permeability ± SEM)		**Mass balance (%) ± SEM**	
		A-B	B-A	Peptide (A-B) treated wells	Peptide (B-A) treated well	A-B	B-A
MDCK-MDR1 (140-170)	CJ-15,208[a]	1.2 ± 0.2	3.4 ± 0.4	1.2 ± 0.2 (4.1 ± 0.6)	1.3 ± 0.1 (4.6 ± 0.1)	93 ± 5	92 ± 8
	[D-Trp]CJ-15,208[b]	1.8 ± 0.2	3.5 ± 0.4	0.68 ± 0.08 (2.8 ± 0.5)	0.89 ± 0.07 (4.9 ± 1.0)	73 ± 5	81 ± 5
MDCK-MDR1 + Inhibitor (140-150)	CJ-15,208 + GF-120918[a]	1.6 ± 0.3	1.7 ± 0.2	1.5 ± 0.1 (5.0 ± 0.1)[b]	1.9 ± 0.1 (7.4 ± 0.5)[b]	77 ± 7	70 ± 8
MDCK-WT (215-410)	CJ-15,208[a]	0.60 ± 0.05	1.5 ± 0.1	0.16 ± 0.01 (0.8 ± 0.1)	0.12 ± 0.05 (0.7 ± 0.1)	95 ± 5	92 ± 3
	[D-Trp]CJ-15,208[a]	2.7 ± 0.1	2.9 ± 0.2	0.22 ± 0.03 (1.0 ± 0.2)	0.23 ± 0.02 (1.3 ± 0.3)	88 ± 8	85 ± 6

Percent permeability calculated from cumulative fraction of LY transported at 60 min. [a]Results presented are mean ± SEM from two or three experiments. [b]Results presented are mean ± SEM from a single experiment.

3.2.2.1 Permeabilities across MDCK-MDR1 cell monolayers

Permeability of CJ-15,208 across MDCK-MDR1 cell monolayers

CJ-15,208 was permeable across MDCK-MDR1 monolayers. It showed P_{app} values of 1.2 ± 0.2 x 10^{-5} cm/sec in the A-B direction and 3.4 ± 0.4 x 10^{-5} cm/sec in the B-A direction (Figure 3.3 and Table 3.1). The value for B-A transport was almost 3 times the value for A-B transport, which suggests that CJ-15,208 could be a substrate for an efflux transporter. To verify whether this was due to P-gp, additional transport studies were conducted in the presence of the P-gp

inhibitor GF-120918. The permeability of CJ-15,208 in the presence of GF-120918 slightly increased in the A-B direction (1.6 ± 0.3 x 10^{-5} cm/sec) and decreased by two-fold in the B-A direction (1.7 ± 0.2 x 10^{-5} cm/sec, Figure 3.4 and Table 3.1). The P_{app} ratio was about 1 in the inhibitor studies, suggesting that GF-120918 was able to inhibit efflux and that CJ-15,208 is likely effluxed to some degree by P-gp.

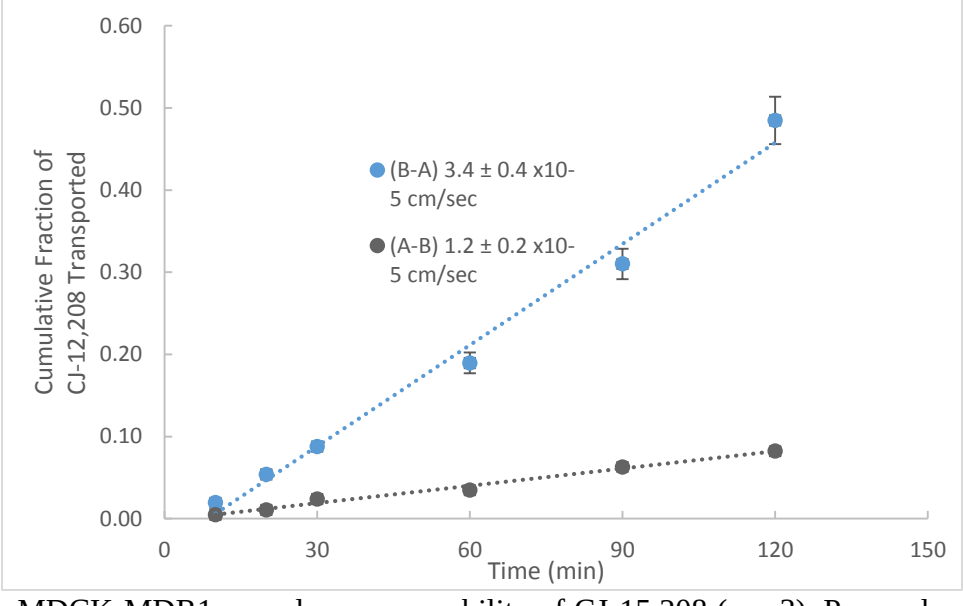

Figure 3.3: MDCK-MDR1 monolayer permeability of CJ-15,208 (n = 3). P_{app} = slope x volume of receiver chamber (cm^3)/area of the filter (cm^2) x 60 (sec), where the volume of receiver chamber = 1.0 mL (A-B) or 0.5 mL (B-A).

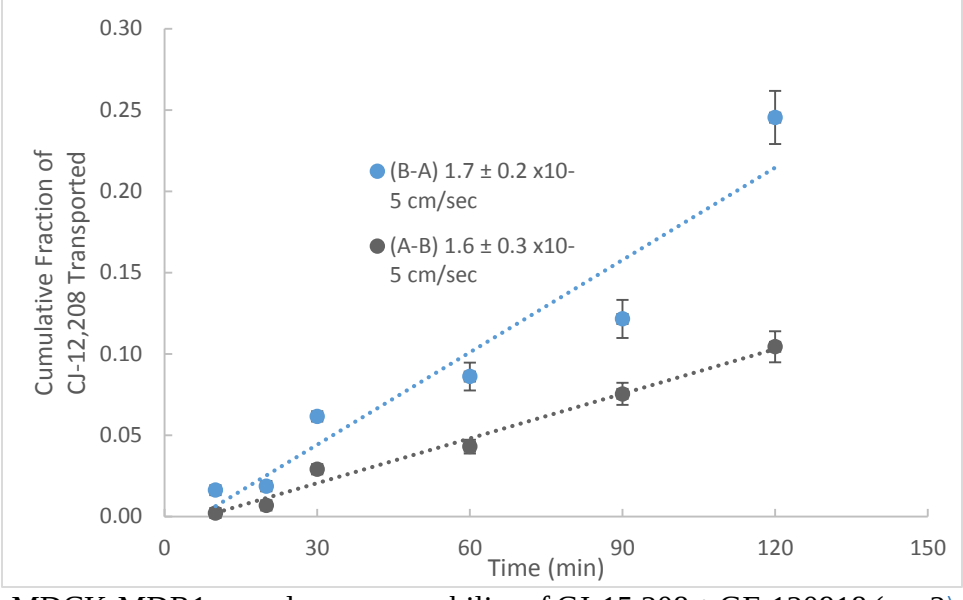

Figure 3.4: MDCK-MDR1 monolayer permeability of CJ-15,208 + GF-120918 (n = 2). P_{app} values were calculated using the formula shown in the legend to Figure 3.3.

The MDCK-MDR1 monolayers showed relatively high permeability of a control (LY) in these experiments with CJ-15,208. Monolayers with and without GF-120918 appeared relatively consistent between wells used for transportation in the A-B and B-A directions, both showing TEER values of >140 Ω/cm^2 for all monolayers and an average LY transport of 1.2 ± 0.2 x 10^{-5} cm/sec (4.1 ± 0.6% permeability over 1 hour) in the wells used to study A-B transport and 1.3 x ± 0.1 10^{-5} cm/sec (4.6 ± 0.1% permeability) in the wells used to study B-A transport without GF-120918 (Figure 3.10 and Table 3.1) and an average LY transport of 1.5 x ± 0.1 10^{-5} cm/sec (5.0 ± 0.1% permeability) in the wells used to study A-B transport and 1.9 ± 0.1 x 10^{-5} cm/sec (7.4 ± 0.5% permeability) in the wells used to study B-A transport with GF-120918 present (Table 3.1). However, these cell monolayers showed lower TEER values and greater LY permeability than those of the MDCK-WT cell monolayers, suggesting that they did not form tight junctions as efficiently. Similar results have been reported by others for MDCK-MDR1 cell monolayers.[13] The average mass balance (± SEM) was 93 ± 5% for the A-B permeability studies and 92 ± 8% for B-

A permeability studies for CJ-15,208 without GF-120918 and 77 ± 7% for the A-B permeability studies and 70 ± 8% for B-A permeability studies for CJ-15,208 with GF-120918 (Table 3.1).

Permeability of [D-Trp]CJ-15,208 across MDCK-MDR1 cell monolayers

[D-Trp]CJ-15,208 was also permeable across MDCK-MDR1 monolayers. It showed a P_{app} value of 1.8 ± 0.2 x 10^{-5} cm/sec in the A-B direction and 3.5 ± 0.4 x 10^{-5} cm/sec in the B-A direction (Figure 3.5 and Table 3.1). The value for B-A transport was almost twice the value for A-B transport which suggests that [D-Trp]CJ-15,208 could be a substrate for an efflux transporter, namely P-gp. However, this study transport was only conducted once, so these results are preliminary.

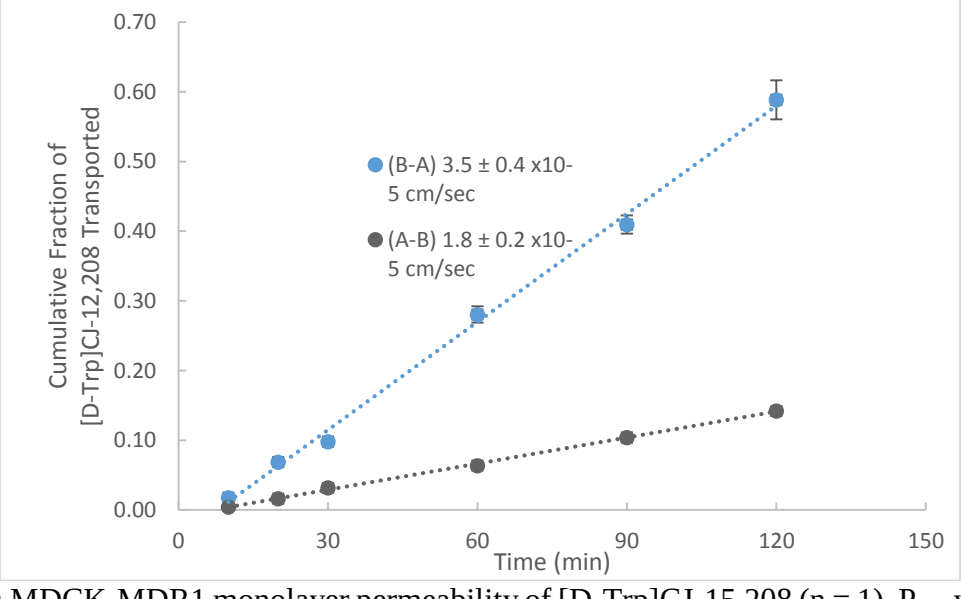

Figure 3.5: MDCK-MDR1 monolayer permeability of [D-Trp]CJ-15,208 (n = 1). P_{app} values were calculated using the formula shown in the legend to Figure 3.3.

The MDCK-MDR1 monolayers also had relatively high permeability to a control in experiments with [D-Trp]CJ-15,208. The monolayers appeared relatively consistent between wells used for transportation in the A-B and B-A directions, both showing TEER values of >140 Ω/cm^2

and average LY of 0.68 ± 0.08 x 10^{-5} cm/sec (2.8 ± 0.5% permeability) in the wells used to study A-B transport and 0.89 ± 0.07 x 10^{-5} cm/sec (4.9 ± 1.0% permeability) in the wells used to study B-A transport (Figure 3.13 and Table 3.1). These are about half of the LY permeabilities observed for the CJ-15,208 studies using MDCK-MDR1 cells. The mass balance (± SEM) was 73 ± 5% for the A-B permeability studies and 81 ± 5% for B-A permeability studies for the D-Trp isomer (Table 3.1).

3.2.2.2 Permeabilities across MDCK-WT cell monolayers

Permeability of CJ-15,208 across MDCK-WT cell monolayers

In this study, MDCK-WT cells also served as a control for efflux by human P-gp. CJ-15,208 was permeable across MDCK-WT monolayers. It showed a P_{app} value of 0.60 ± 0.05 x 10^{-5} cm/sec in the A-B direction and 1.5 ± 0.1 x 10^{-5} cm/sec in the B-A direction (Figure 3.6 and Table 3.1). The value for B-A transport was about 2.5 times the value for A-B transport which suggests that CJ-15,208 is a substrate for an endogenous efflux transporter.

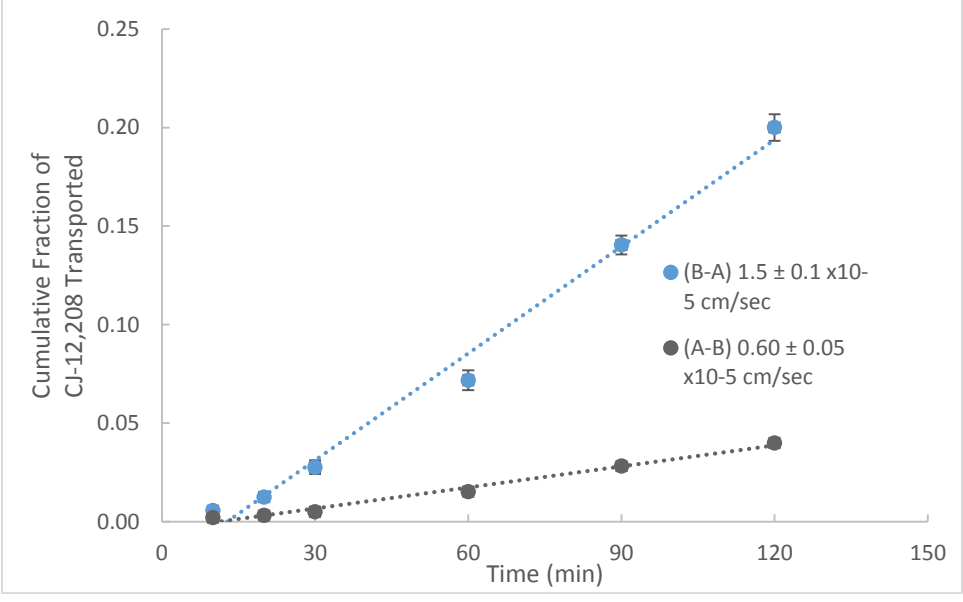

Figure 3.6: MDCK-WT monolayer permeability of CJ-15,208 (n = 2). P_{app} values were calculated using the formula shown in the legend to Figure 3.3.

The MDCK-MDR1 and MDCK-WT cells were examined for P-gp expression using western blot analysis with an antibody with affinity for human and canine P-gp, and no P-gp expression was detected in the MDCK-WT cells (Figures 3.7 and 3.8). However, efflux by canine P-gp in MDCK-WT cells was not examined using inhibitors in the these studies, and canine P-gp has been detected in MDCK-WT cells using a higher concentration of the antibody.[16] Canine forms of MRP efflux proteins has also been detected in MDCK cells,[16, 17] and one study suggests that they can be more highly expressed in MDCK-MDR1 cells than wild type cells.[16] It has been shown that transfection with the human MDR1 gene can affect the expression of endogenous MDCK transport proteins,[16] so another unidentified efflux protein may be effecting these results. Inhibitor studies[18] are required to determine what efflux proteins may be involved in the observed efflux in the WT cells. Since the P_{app} ratios of CJ-15,208 across MDCK-MDR1 cells and MDCK-WT cells are similar, it is unclear from these studies if human P-gp is involved in its efflux.

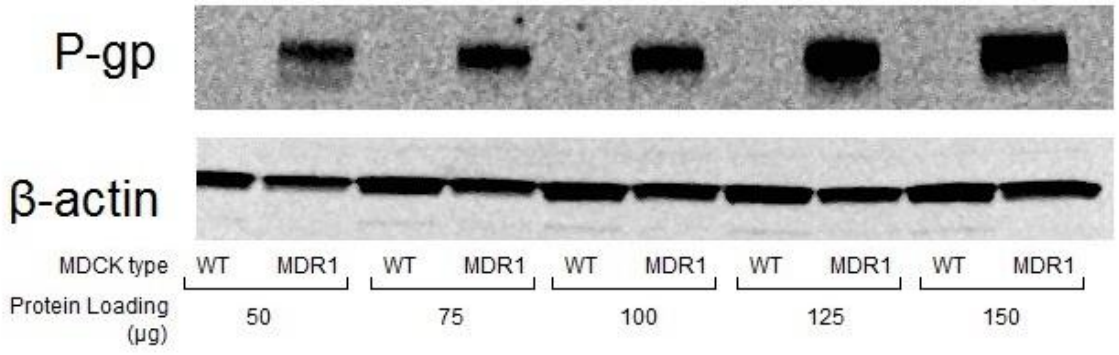

Figure 3.7: Western blot of P-gp in MDCK-WT and MDR1 cells following 6 days in culture.

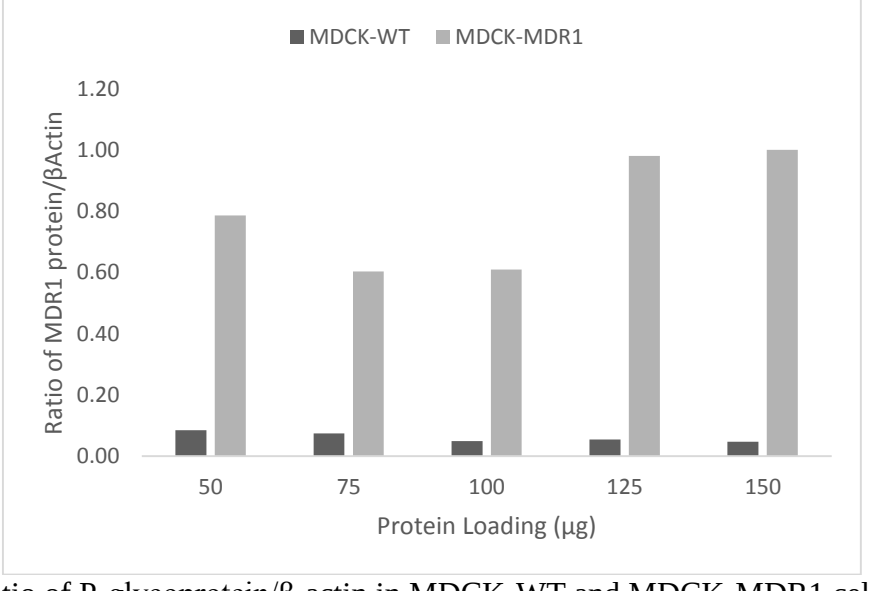

Figure 3.8: Ratio of P-glycoprotein/β-actin in MDCK-WT and MDCK-MDR1 cells as measured by Western blot analysis.

The MDCK-WT monolayers appeared consistent between wells used for transportation in the A-B and B-A directions, both showing TEER values of >200 Ω/cm^2 and an average LY of 0.22 ± 0.03 x 10^{-5} cm/sec (0.8 ± 0.1% permeability) in the wells used to study A-B transport and 0.23 ± 0.02 x 10^{-5} cm/sec (0.7 ± 0.1% permeability) in the wells used to study B-A transport (Table 3.1). The mass balance (± SEM) was 95 ± 5% for the A-B permeability studies and 92 ± 3% for B-A permeability studies for the L-Trp isomer (Table 3.1).

Permeability of [D-Trp]CJ-15,208 across MDCK-WT cell monolayers

In MDCK-WT monolayers, [D-Trp]CJ-15,208 showed a permeability of 2.7± 0.1 x 10^{-5} cm/sec in the A-B direction and 2.9 ± 0.2 x 10^{-5} cm/sec in the B-A direction (Figure 3.9 and Table 3.1). The value for B-A transport was equal to the value for A-B transport which suggests that [D-Trp]CJ-15,208 is a not substrate for an endogenous efflux transporter in these cells. The MDCK-WT monolayers appeared consistent between wells used for transportation in the A-B and B-A directions, both showing TEER values of >200 Ω/cm^2 and an average LY of 0.22 ± 0.03 x 10^{-5} cm/sec (1.0 ± 0.2% permeability) in the wells used to study A-B transport and 0.23 ± 0.02 x 10^{-5} cm/sec (1.3 ± 0.3% permeability) in the wells used to study B-A transport (Table 3.1). The mass balance (± SEM) was 88 ± 8% for the A-B permeability studies and 85 ± 6% for B-A permeability studies for the D-Trp isomer (Table 3.1).

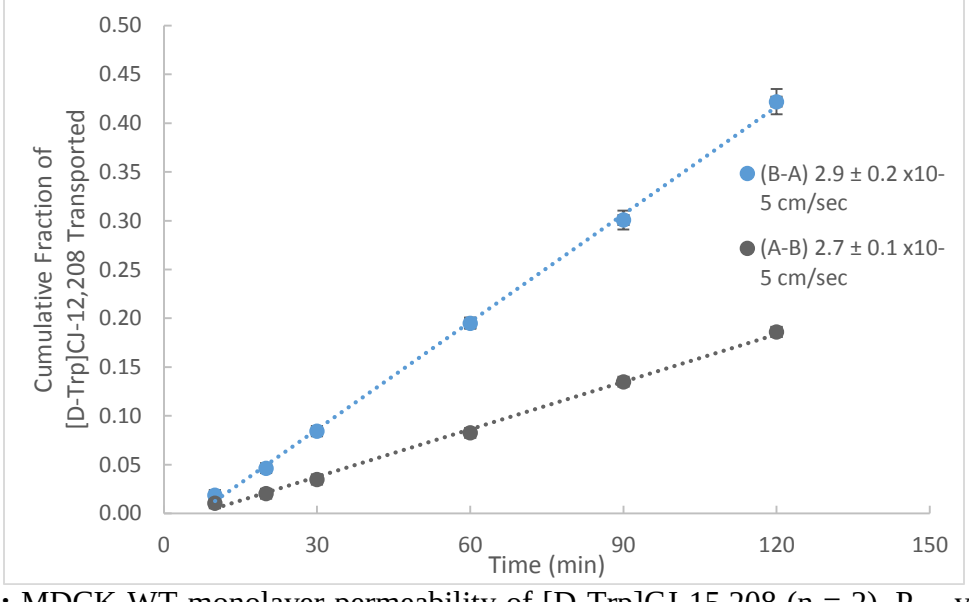

Figure 3.9: MDCK-WT monolayer permeability of [D-Trp]CJ-15,208 (n = 2). P_{app} values were calculated using the formula shown in the legend to Figure 3.3.

3.2.3 Potential for active transport

A short lag of about 10 min was detected between the time when either peptide was added to the monolayer and when transport was observed in both MDCK-WT and MDCK-MDRI studies (Figures 3.3-3.6 and 3.9), suggesting that these peptides may be actively transported. A similar 10 min lag time was observed across Caco-2 cells.[3] Kinetic studies with varying temperatures could be conducted to examine this hypothesis.[19]

3.3 Conclusions and future directions

These preliminary results suggest that CJ-15,208 interacts with and is effluxed by efflux protein(s), but the similar P_{app} ratios observed across both MDCK-MDR1 and MDCK-WT cell monolayers make it unclear which efflux proteins are involved. The efflux is eliminated in the presence of GF-120918, however this inhibitor has been shown to eliminate efflux by endogenous canine efflux proteins in MDCK-WT cells as well.[20] Further, GF-120918, which is also a potent inhibitor of the breast cancer related protein (BCRP)[21] as well as MDR1, was not used in these MDCK-WT transport studies. It is possible that CJ-15,208 may be effluxed by other proteins expressed in MDCK-WT cells, including canine isoforms of P-gp[17] or MRP2,[16] suggesting further studies using different inhibitors. While P-gp was not detected in the MDCK-WT cells using Western blot analysis, other studies have detected P-gp in MDCK-WT cells using a higher concentration of P-gp antibody.[16] There was no evidence of efflux of [D-Trp]CJ-15,208 across MDCK-WT cell monolayers, but a P_{app} ratio of 2 in a preliminary study suggested possible efflux across MDCK-MDR1 cells. Additional studies are required to confirm these results, and inhibitor studies[22] can be used to determine what efflux proteins may be involved. Lag times in the transport of both of these peptides suggest the possibility of active transport, possible via endocytosis.[23]

Permeability studies of [D-Trp]CJ-15,208 across MDCK-MDR1 cell monolayers should be repeated, and GF-120918 could be used to determine whether any observed efflux is due to canine P-gp in MDCK-WT cells (BCRP has been reported to be low in these cells[16]). Additionally, these experiments could be repeated with lower concentrations (< 5 μM) of either peptide. Efflux proteins have been shown to be saturable,[24] and 50 μM may be too high a concentration to observe efflux by proteins with lower expression or activity in these cell lines. Carrier-mediated transport could also be assessed using variable temperature studies.[24]

3.4 Experimental section

3.4.1 Materials and instrumentation

Dulbecco's modified Eagle's medium (DMEM) was obtained from Gibco (Grand Island, NY), and fetal bovine serum (FBS) was obtained from Atlanta Biologics (Lawrenceville, GA). Non-essential amino acids, penicillin and streptomycin were purchased from Cellgro (Manassas, VA). HBSS, pH 7.4, colchicine, lucifer yellow, Elacridar (GF-120918), protein standard, monoclonal anti-β-actin antibody, Tris base, ethylenediaminetetraacetic (EDTA), ethylene glycol tetraacetic acid (EGTA), sodium dodecyl sulfate (SDS), sodium chloride (NaCl), sodium deoxycholate, phenylmethanesulfonyl fluoride (PMSF), DMA, TWEEN-20, and TritonX100 were purchased from Sigma-Aldrich (St. Louis, MO), and polycarbonate transwell filters and polystyrene plates were obtained from Costar (Corning, NY). C219 mouse monoclonal antibody A to P-glycoprotein was purchased from Covance (Princeton, NJ). Horseradish peroxidase-conjugated anti-mouse secondary antibody was purchased from Jackson ImmunoResearch Inc. (West Grove, PA). Dimethyl sulfoxide (DMSO, molecular biology grade), sodium pyruvate, sodium bicarbonate, HEPES, glycine, (±)-verapamil hydrochloride, a BCA protein assay reagent kit, and protease inhibitor cocktail (PI-78441) were purchased from Thermo Fisher Scientific

(Waltham, MA). Criterion precast gels, 4-20% Tris-HCl, 1.0 mm, 1X Tris-Glycine SDS running buffer, 4x Laemmli sample buffer, protein standard (161-0374), and SuperSignal West Pico Chemiluminescence substrate were purchased from Bio-Rad Laboratories, Inc. (Hercules, CA). Immoblion-P polyvinylidene difluoride (PVDF), 0.45um pore, membranes were purchased from Millipore (Billerica, MA). Rhodamine 123 was purchased from MP Biomedicals, LLC (Santa Ana, CA). CJ-14,280 and [D-Trp]CJ-15,208 were synthesized and purified by Dr. Sanjeewa N. Senadheera.[25]

A SpectraMax M5 microplate fluorometer (Molecular Devices, Sunnyvale) was used for analysis of LY transport. A Synergy HT microplate reader (BioTek, Winooski, VT) was used for analysis of Rh 123 efflux and protein concentration. LC-MS/MS analysis of peptide concentration in the peptide transport study was performed on an Acquity Ultra Performance liquid chromatography (UPLC) system coupled to a Quattro mass spectrometer (Waters, Milford) in the University of Kansas Mass Spectroscopy Laboratory.

3.4.2 Cell culture

MDCK-WT and MDCK-MDR1 cells (obtained from Dr. P. Borst, the Netherlands Cancer Institute, Amsterdam, passage 62-70) were grown in a humidified incubator at 37 ^{o}C under 5% CO_2 in air in Dulbecco's modified Eagle's medium (DMEM) containing 10% heat inactivated FBS, 0.1 mM nonessential amino acids, 2 mM L-glutamine, 100 U/mL penicillin, and 100 µg/mL streptomycin. MDCK-MDR1 cells were grown in the presence of 80 ng/mL colchicine. MDCK cells were seeded on polycarbonate transwells (0.4 µM pore size, 12 mm diameter, Costar #3401) or 24 well plates at a density of 50,000 cells/cm^2 and grown for 6 days. Cell culture media was replaced every other day.

3.4.3 Immunoblotting

Western blot analysis was performed to detect P-gp protein expression. Six days after seeding, the cells were trypsinized by the addition of 1.5 mL trypsin which was aspirated out after ten seconds, and the cells then incubated at 37^{o}C for 5 min. The cells were then resuspended in ice-cold DPBS and pelleted by centrifugation (1,500 RPM for 10 min). The pellets were lysed in RIPA buffer (10 mM Tris-Cl (pH 8.0), 1 mM EDTA, 0.5 mM EGTA, 1% Triton X-100, 0.1% sodium deoxycholate, 0.1% SDS, and 140 mM NaCl; 1 mM PMSF was added immediately before use), incubated at 4 ^{o}C for 20 min with occasional vortexing, transferred to eppendorf tubes, and centrifuged at 1,320 RPM for 15 min. The protein concentration of the supernatant was determined using a BCA protein assay reagent kit. To insure detection of any low-level expression of P-gp in MDCK-WT cells, 50-150 μg of total cellular protein were used for Western blotting. The samples and a protein standard were diluted with 4x Laemmli sample buffer (277.8 mM Tris-HCl, pH 6.8, 4.4% lithium dodecyl sulfate (LDS), 44.4% (w/v) glycerol, and 0.02% bromophenol blue). The samples were then analyzed by electrophoresis on a Criterion precast gel, 4-20% Tris-HCl, 1.0 mm, with a 1X Tris-glycine SDS running buffer. The proteins were transferred onto Immoblion-PVDF 0.45 um pore membranes in transfer buffer (48 mM Tris, 39 mM glycine pH 9.2, and 1.3 mM SDS) using a Trans-Blot SD semi-dry transfer cell (Bio-Rad Laboratories, Inc., Hercules, CA) at 10V+ overnight.

After transfer membranes were blocked for one hour at room temperature in blocking solution [3% bovine serum albumin (BSA) and 0.1% TWEEN-20 in Tris-buffered saline (TBS, 0.025 M Tris, pH 7.5, 0.15 M NaCl)]. Membranes were then incubated overnight at 4 ^{o}C with C219 (anti-P-gp) mouse monoclonal antibody A (1:1,000 dilution in 15 mL blocking solution) or monoclonal anti-β-actin antibody produced in mouse (1:3,000 dilution in 15 mL blocking solution). The membranes were then washed with 0.3% Tween-20 in TBS 3 times for 20 min each.

Next, membranes were incubated for 45 min at room temperature with secondary antibody, horseradish peroxidase-conjugated anti-mouse antibody (1:5,000 dilution in 15 mL blocking solution). The membranes were washed again as previously described. Chemiluminescence signals of protein bands were detected using SuperSignal West Pico Chemiluminescence substrate. The intensity of the chemiluminescence signals for the proteins were determined using a Kodak Image Station 4000R imager, and protein band intensity was quantified by ImageJ software (NIH, Bethesda, MD).

3.4.4 Rhodamine 123 efflux experiments

MDCK–MDR1 cell monolayers were washed twice with 500 µL HBSS, and pre-incubated with CJ-15,208 (in 2.25% DMA and 0.25% DMSO in HBSS, vehicle 1) or [D-Trp]CJ-15,208 (in 1% DMSO in HBSS), 0-50 µM, for 30 min at 37°C. Verapamil (600 µM) in vehicle 1 was used as a positive control. The monolayers were then incubated with 5 µM rhodamine 123 at 37 °C for 60 min, washed with ice-cold phosphate-buffered saline (PBS, 2 x 500 µL) and lysed with 200 µL ice-cold 1% Triton X100 in PBS. Fluorescence (excitation 497 nm, emission 526 nm) was measured and protein concentration in the cell lysate was determined using the BCA assay. Relative fluorescence units (RFU) were calculated as follows:

$$RFU = (Fluorescence_{comp} - Fluorescence_{background})/\text{protein concentration (mg/mL)}$$

3.4.5 Standard curves of the low permeability standard lucifer yellow (LY)

The standard curve of LY was obtained in HBSS ranging over a range of concentrations (1-100 µM) and displayed linearity ($r^2 = 0.9998$, Figure 3.10). The solutions of LY (200 µL) were

analyzed using a 96 well fluorescence plate reader (excitation 485 nm, emission wavelength 538 nm).

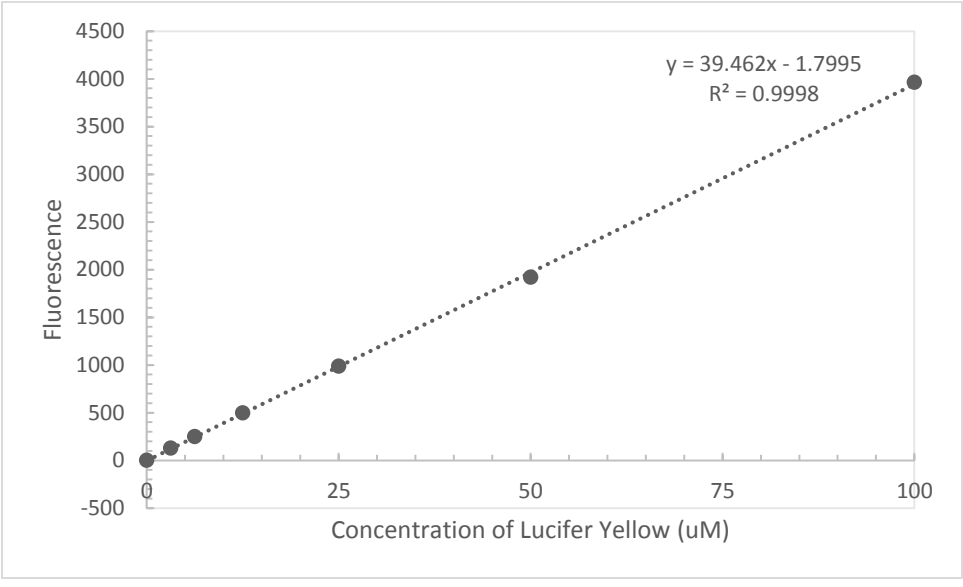

Figure 3.10: Representative standard curve for LY

3.4.6 Transport experiments

The integrity of the cell monolayers was examined by measuring TEER values and the transport of the low paracellular permeability standard LY. The TEER values were corrected by subtracting background values for the filters. The criteria to use the cell monolayers for transport studies for MDCK-WT monolayers were TEER values of >200 Ω/cm^2 and a P_{app} values for LY of $\leq 0.5 \times 10^{-5}$ cm/sec.[11, 12] The criteria to use the cell monolayers for transport studies for MDCK-MDR1 monolayers were TEER values of >140 Ω/cm^2 and a P_{app} values for LY of $\leq 1.5 \times 10^{-5}$ cm/sec (MDCK-MDR1), and $\leq 2.5 \times 10^{-5}$ cm/sec (MDCK-MDR1 + GF-120918).[13] The filters containing cell monolayers were washed twice with HBSS, pH 7.4, at 37 ºC. For assessment of monolayer integrity of the cells, HBSS on the apical side was replaced with LY (0.5 mL of 100

μM solution in HBSS). The LY transport to evaluate cell monolayer integrity was performed during the 3rd h after the initial 2 h peptide transport experiment. The experiment was performed in duplicate or triplicate for 60 min with aliquots (200 μL) taken at 15, 30, 45, and 60 min from the basolateral side. At every time point an aliquot was removed it was replaced by an equal amount of HBSS to maintain constant volume. The samples were analyzed using a 96 well fluorescence plate reader (see Materials). Examples of LY transport in MDCK-MDR1 and MDCK-WT cells can be seen in Figures 3.11 and 3.12, respectively.

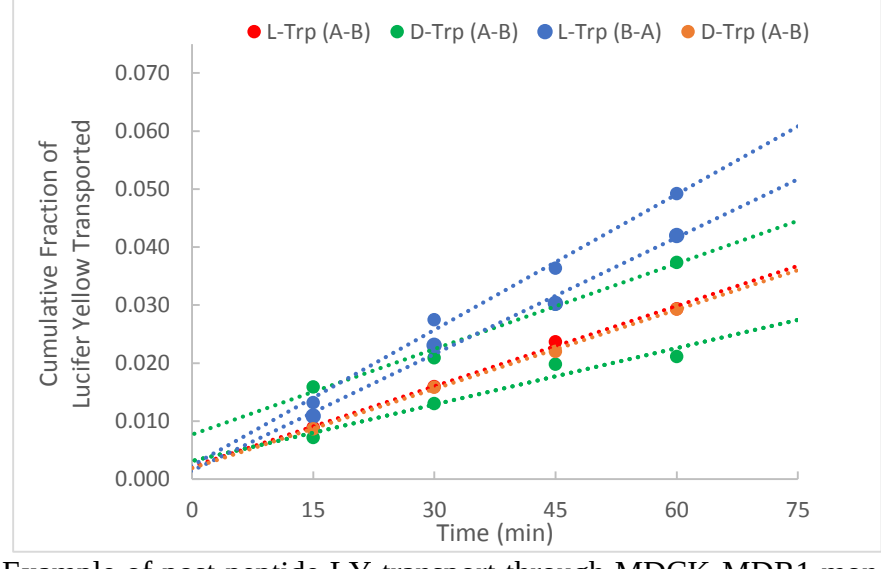

Figure 3.11: Example of post peptide LY transport through MDCK-MDR1 monolayers. Wells were treated with CJ-15,208 (L-Trp peptide) in vehicle 1 or [D-Trp]CJ-15,208 (D-Trp peptide) in 1% DMSO in HBSS for the initial 2 h, and LY transport was then carried out in the wells during the 3rd h.

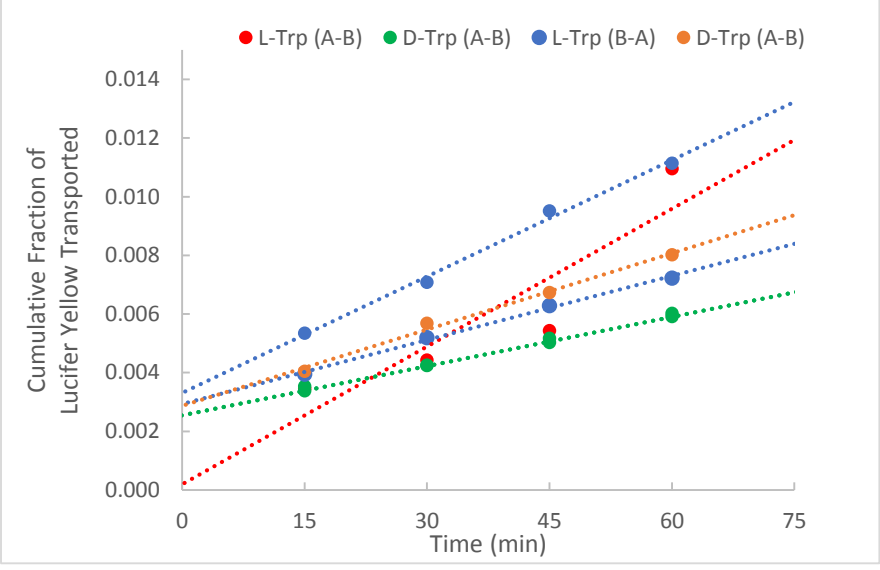

Figure 3.12: Example of post peptide LY transport through MDCK-WT monolayers. Wells were treated with CJ-15,208 (L-Trp peptide) in vehicle 1 or [D-Trp]CJ-15,208 (D-Trp peptide) in 1% DMSO in HBSS for the initial 2 h, and LY transport was then carried out in the wells during the 3rd h.

Transport experiments for the peptides were performed similarly to the procedure described above for LY. For experiments utilizing the P-gp inhibitor GF-120918, the MDCK-MDR1 cell monolayers were incubated with the P-gp inhibitor (5 μM) in the appropriate vehicle in the donor side for 20 min before the peptides were added. Transport in the A-B and B-A directions was performed in duplicate or triplicate and monitored by the collection of aliquots at 10, 20, 30, 60, 90, and 120 min. At every time point an aliquot was removed it was replaced by an equal amount of HBSS to maintain constant volume. Early time points were taken to monitor any initial lag in the transport of the two peptides. The working concentration used for both CJ-15,208 and [D-Trp]CJ-15,208 was 50 μM in vehicle 1 and 1% DMSO in HBSS, respectively. Aliquots of the donor compartment were taken at the beginning and the end of the experiments. The peptide concentrations were determined by LC-MS/MS (see below).

3.4.7 LC-ESI-MS/MS analysis

Sample preparation for CJ-15,208 and [D-Trp]CJ-15,208

The samples from the transport studies of CJ-15,208 and [D-Trp]CJ-15,208 were stored at 0 ^{o}C immediately after the experiments. Following thawing, the internal standard *cyclo*[L-Phe-*N*-Me-D-Ala-L-Phe-Trp] (20 μL of a 12.5 μM solution in MeCN) was added to 80 μL of the transport samples. The samples were vortexed and stored in glass vials to prevent the hydrophobic macrocyclic peptides from absorbing onto the sides of plastic containers.

LC-MS/MS method for CJ-15,208 and [D-Trp]CJ-15,208

LC-MS/MS analysis was performed by Dr. Tanvir Khaliq and by staff from the University of Kansas Mass Spectroscopy Laboratory. Liquid chromatography was performed on a Hypersil BDS C8 column (3 μ, 2.1 mm × 50 mm). Sample injection volume was 20 μL, and analysis was conducted using a gradient on a Waters Acquity Classic UPLC (Waters Corp., Milford MA) at a flow rate of 0.27 mL/min. Peptides were separated using a gradient of water (solvent A) and acetonitrile (solvent B), both containing 0.08% formic acid, as follows: 0-2 min (20% B), 2-3 min (20-50% B), 3-6 min (50-80% B), 6-7 min (80% B), 7-8 min (80-20% B) and 8-10 min (20% B). The retention times for CJ-15,208 and [D-Trp]CJ-15,208 were 3.8 min and 6.4 min, respectively, and the retention time of the IS was 4.5 min.

The UPLC was coupled to a triple quadrupole mass spectrometer (Quattro Ultima Micromass Ltd., Manchester UK) operating in the positive-ion mode. Cone voltage and collision induced dissociation conditions for precursor/product ion pairs of CJ-15,208 or [D-Trp]CJ-15,208 and its internal standard were determined by post column mixing of standards infused under UPLC elution conditions. Data acquisition was carried out with Mass Lynx 4.1 software with the following settings: capillary voltage, 2.8 kV; cone voltages, 80 V IS, 30V analytes; source temperature, 100 °C; desolvation temperature, 220 °C; cone gas flow, 280 L/h; desolvation gas

flow, 1200 L/h. Q1 and Q3 resolution were 0.8 u FWHH. The argon filled collision cell pressure was 3.35 × 10^{-3} mbar on a gauge in-line with the cell. MRM was used for CJ-15,208 and [D-Trp]CJ-15,208: $[M + H]^+$ *m/z* 578.1 → 217.1 and 245.0, collision energy 30 eV and for the internal standard $[M + H]^+$ *m/z* 566.2 → 232.9 (Figure 3.13), collision energy 22 eV, with a dwell time of 0.3 s. The standard curve for the L-Trp isomer was obtained from 0.1 μM to 25 μM and displayed linearity (r^2 = 0.9733, Figure 3.14). The standard curve for the D-Trp isomer was obtained from 0.1 μM to 25 μM and displayed polynomial correlation (r^2 = 0.9867, Figure 3.15). The transport samples were analyzed using the same conditions as the standards.

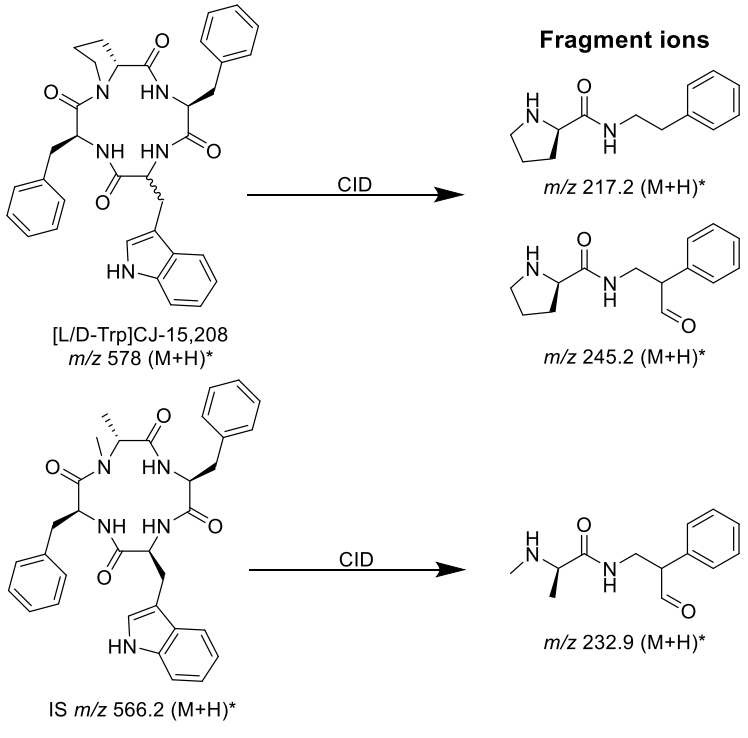

Figure 3.13: Mass spectral fragmentation of the macrocyclic tetrapeptides

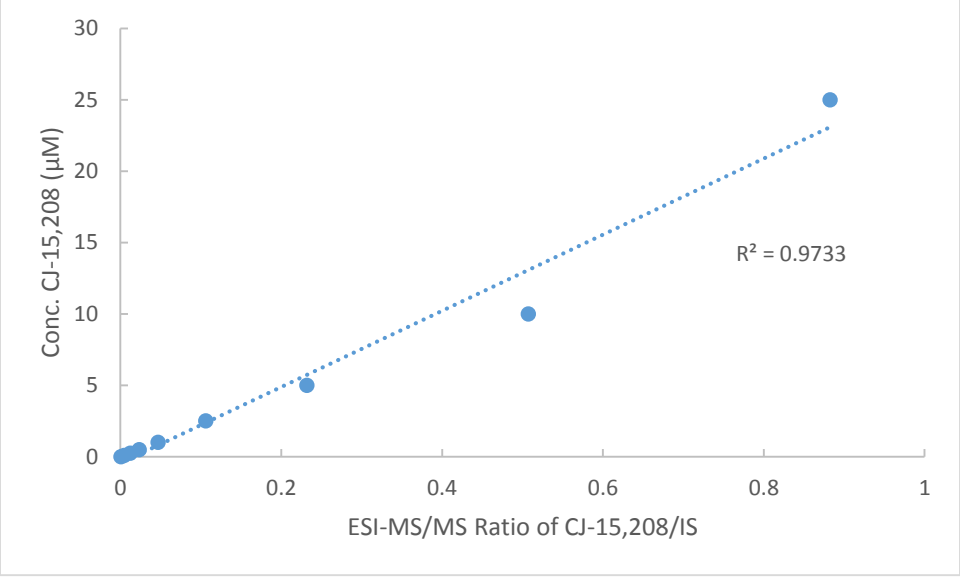

Figure 3.14: Representative standard curve of CJ-15,208 by LC-MS/MS used for quantifying the peptide in MDCK monolayer transport studies.

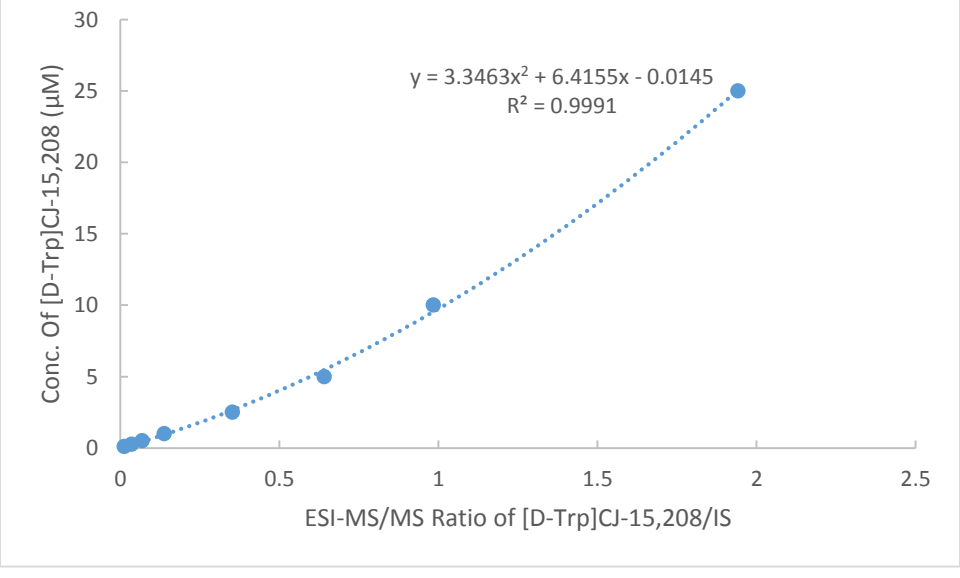

Figure 3.15: Representative standard curve of [D-Trp]CJ15,208 by LC-MS/MS used for quantifying the peptide in MDCK monolayer transport studies.

3.4.8 P_{app} and percent permeability calculations

The cumulative fraction of the drug transported at each time point was calculated by dividing the concentration in the receiver at each time point, following correction for aliquot removal (by addition of an equal volume of HBSS), by the donor concentration (concentration of the drug at time = 0). The cumulative fraction transported was plotted vs. time to obtain the slope of the line (flux). The P_{app} value was then calculated from the following formula:

P_{app} = slope x volume of receiver chamber (cm^3)/area of the filter (cm^2) x 60 (sec)

The cumulative fraction of LY transported at 60 min was used to calculate percent permeability.

3.5 References

1. Aldrich, J. V.; Senadheera, S. N.; Ross, N. C.; Ganno, M. L.; Eans, S. O.; McLaughlin, J. P. The macrocyclic peptide natural product CJ-15,208 is orally active and prevents reinstatement of extinguished cocaine-seeking behavior. *J Nat Prod* **2013,** 76, 433-8.

2. Eans, S. O.; Ganno, M. L.; Reilley, K. J.; Patkar, K. A.; Senadheera, S. N.; Aldrich, J. V.; McLaughlin, J. P. The macrocyclic tetrapeptide [D-Trp]CJ-15,208 produces short-acting kappa opioid receptor antagonism in the CNS after oral administration. *Br J Pharmacol* **2013,** 169, 426-36.

3. Joshi, A. Synthesis and biological evaluation of dynorphin analogs and, Caco-2 permeability of opioid macrocyclic tetrapeptides. Ph.D Dissertation, University of Kansas, Lawrence, KS, 2013.

4. Sjostedt, N.; Kortejarvi, H.; Kidron, H.; Vellonen, K. S.; Urtti, A.; Yliperttula, M. Challenges of using in vitro data for modeling P-glycoprotein efflux in the blood-brain barrier. *Pharm Res* **2014,** 31, 1-19.

5. Meunier, V.; Bourrie, M.; Berger, Y.; Fabre, G. The human intestinal epithelial cell line Caco-2; pharmacological and pharmacokinetic applications. *Cell Biol Toxicol* **1995,** 11, 187-94.

6. Volpe, D. A. Drug-permeability and transporter assays in Caco-2 and MDCK cell lines. *Future Med Chem* **2011,** 3, 2063-77.

7. Braun, A.; Hammerle, S.; Suda, K.; Rothen-Rutishauser, B.; Gunthert, M.; Kramer, S. D.; Wunderli-Allenspach, H. Cell cultures as tools in biopharmacy. *Eur J Pharm Sci* **2000,** 11 Suppl 2, S51-60.

8. Passeleu-Le Bourdonnec, C.; Carrupt, P. A.; Scherrmann, J. M.; Martel, S. Methodologies to assess drug permeation through the blood-brain barrier for pharmaceutical research. *Pharm Res* **2013,** 30, 2729-56.

9. Hakkarainen, J. J.; Jalkanen, A. J.; Kaariainen, T. M.; Keski-Rahkonen, P.; Venalainen, T.; Hokkanen, J.; Monkkonen, J.; Suhonen, M.; Forsberg, M. M. Comparison of in vitro cell models in predicting in vivo brain entry of drugs. *Int J Pharm* **2010,** 402, 27-36.

10. Ouyang, H.; Andersen, T. E.; Chen, W.; Nofsinger, R.; Steffansen, B.; Borchardt, R. T. A comparison of the effects of P-glycoprotein inhibitors on the blood-brain barrier permeation of cyclic prodrugs of an opioid peptide (DADLE). *J Pharm Sci* **2009,** 98, 2227-36.

11. Kauffman, A. L.; Gyurdieva, A. V.; Mabus, J. R.; Ferguson, C.; Yan, Z.; Hornby, P. J. Alternative functional in vitro models of human intestinal epithelia. *Front Pharmacol* **2013,** 4, 79.

12. Madgula, V. L.; Avula, B.; Reddy, V. L. N.; Khan, I. A.; Khan, S. I. Transport of decursin and decursinol angelate across Caco-2 and MDR-MDCK cell monolayers: in vitro models for intestinal and blood-brain barrier permeability. *Planta Med* **2007,** 73, 330-5.

13. Hellinger, É. Prediction of intestinal absorption and brain penetration of drugs. Ph.D Dissertation, Semmelweis University, Budapest, 2012.

14. Patel, M.; Mandava, N. K.; Pal, D.; Mitra, A. K. Amino acid prodrug of quinidine: an approach to circumvent P-glycoprotein mediated cellular efflux. *Int J Pharm* **2014,** 464, 196-204.

15. Tang, F.; Ouyang, H.; Yang, J. Z.; Borchardt, R. T. Bidirectional transport of rhodamine 123 and Hoechst 33342, fluorescence probes of the binding sites on P-glycoprotein, across MDCK-MDR1 cell monolayers. *J Pharm Sci* **2004,** 93, 1185-94.

16. Kuteykin-Teplyakov, K.; Luna-Tortós, C.; Ambroziak, K.; Löscher, W. Differences in the expression of endogenous efflux transporters in MDR1-transfected versus wildtype cell lines affect P-glycoprotein mediated drug transport. *Br J Pharmacol* **2010,** 160, 1453-1463.

17. Gartzke, D.; Fricker, G. Establishment of optimized MDCK cell lines for reliable efflux transport studies. *J Pharm Sci* **2014,** 103, 1298-1304.

18. Augustijns, P. F.; Bradshaw, T. P.; Gan, L. S.; Hendren, R. W.; Thakker, D. R. Evidence for a polarized efflux system in CACO-2 cells capable of modulating cyclosporin A transport. *Biochem Biophys Res Commun* **1993,** 197, 360-5.

19. Liu, H.; Yu, N.; Lu, S.; Ito, S.; Zhang, X.; Prasad, B.; He, E.; Lu, X.; Li, Y.; Wang, F.; Xu, H.; An, G.; Unadkat, J. D.; Kusuhara, H.; Sugiyama, Y.; Sahi, J. Solute carrier family of the organic anion-transporting polypeptides 1A2- Madin-Darby canine kidney II: a promising in vitro system to understand the role of organic anion-transporting polypeptide 1A2 in blood-brain barrier drug penetration. *Drug Metab Dispos* **2015,** 43, 1008-18.

20. Tang, F.; Horie, K.; Borchardt, R. T. Are MDCK cells transfected with the human MDR1 gene a good model of the human intestinal mucosa? *Pharm Res* **2002,** 19, 765-72.

21. Nakanishi, T.; Ross, D. D. Breast cancer resistance protein (BCRP/ABCG2): its role in multidrug resistance and regulation of its gene expression. *Chinese J Cancer* **2012,** 31, 73-99.

22. Wang, Q.; Strab, R.; Kardos, P.; Ferguson, C.; Li, J.; Owen, A.; Hidalgo, I. J. Application and limitation of inhibitors in drug-transporter interactions studies. *Int J Pharm* **2008,** 356, 12-8.

23. Terasaki, T.; Hirai, K.; Sato, H.; Kang, Y. S.; Tsuji, A. Absorptive-mediated endocytosis of a dynorphin-like analgesic peptide, E-2078 into the blood-brain barrier. *J Pharmacol Exp Ther* **1989,** 251, 351-7.

24. Sugano, K.; Kansy, M.; Artursson, P.; Avdeef, A.; Bendels, S.; Di, L.; Ecker, G. F.; Faller, B.; Fischer, H.; Gerebtzoff, G.; Lennernaes, H.; Senner, F. Coexistence of passive and carrier-mediated processes in drug transport. *Nat Rev Drug Discovery* **2010,** 9, 597-614.

25. Senadheera, S. N.; Kulkarni, S. S.; McLaughlin, J. P.; Aldrich, J. V. Improved synthesis of CJ-15,208 isomers and their pharmacological activity at opioid receptors. In: Lebl M, editor. Building Bridges: *Proc 22nd Amer Pept Symp San Diego, CA* **2011**, 346–347.